A PHOTOGRAPHIC INVESTIGATION
OF
SATURATED NUCLEATE BOILING

By

DOUGLAS LEONARD JEFFERY ANDERSON

A Thesis

Submitted to the Faculty of Graduate Studies

in Partial Fulfilment of the Requirements

for the Degree

Master of Engineering

McMaster University

October 1969

MASTER OF ENGINEERING (1969) McMASTER UNIVERSITY
(Mechanical Engineering) Hamilton, Ontario

TITLE: A Photographic Investigation of Saturated Nucleate Boiling

AUTHOR: Douglas L. J. Anderson, B.Eng. (General Motors Institute)

SUPERVISOR: Dr. Ross L. Judd

NUMBER OF PAGES: xii - 103

SCOPE AND CONTENTS:

This thesis describes a photographic investigation of saturated nucleate boiling. Five different fluids were boiled on an oxide coated glass surface at various levels of heat flux. The nature of the boiling surface was such that the boiling phenomenon could be photographed through the surface from below.

Active nucleation sites were identified and counted by analysis of still photographs obtained using this technique. Active nucleation site density data obtained from the analysis was correlated with surface temperature using the Gaertner site activation theory

$$\frac{N}{A} = N_o \exp\left\{ - \left(\frac{16\pi\sigma^3 M^2 N^*}{3\rho_L{}^2 R^3 [\ln(\frac{P_\infty}{P_v})]^2} \right) \Phi \left(\frac{1}{T_w}\right)^3 \right\}$$

which requires the use of two arbitrary constants N_o and Φ.

It is demonstrated that for the particular surface used, the product

$$\left(\frac{16\pi\sigma^3 M^2 N^*}{3\rho_L^2 R^3 [\ln(\frac{P_\infty}{P_v})]^2} \right) \Phi = 3.305 \times 10^9 \, ^\circ K^3$$

irrespective of the fluid boiled so that the relationship

$$\frac{N}{A} = N_o \exp \left\{ -3.305 \times 10^9 \left(\frac{1}{T_w}\right)^3 \right\}$$

satisfactorily predicts the active nucleation site density.

ACKNOWLEDGEMENTS

The author is indebted to many people for their co-operation and assistance throughout the investigation and the preparation of this thesis. Grateful acknowledgement is given to Dr. Ross L. Judd who provided guidance and advice in planning and performing the experimental phases of the project and who in addition reviewed the manuscript and provided many worthwhile suggestions.

The author also expresses his appreciation to Messrs. Gunnar Liepins and Robert J. Clements and their staffs at General Motors of Canada for their assistance in co-ordinating the many technical and financial arrangements of the program.

Technical assistance was gratefully received from Mr. Uldes Golts and Mr. John Watson of the Photographic Facility, Mr. Robert Brown and Mr. John Crooks of the Mechanical Engineering Department, and the staff of the Engineering Machine Shop, all at McMaster University.

This project was supported by General Motors of Canada and National Research Council Grant A4362 under the terms of the Bachelor-Master Program administered jointly by General Motors of Canada, General Motors Institute, and McMaster University.

TABLE OF CONTENTS

Table Of Contents (Continued)

LIST OF ILLUSTRATIONS

List Of Illustrations (Continued)

LIST OF TABLES

LIST OF APPENDICES

NOMENCLATURE

Term	Definition	Units
A	Heater surface area.	square feet
B	Constant of correlation by Kurihara and Myers based on liquid properties.	———
C	Specific heat of saturated liquid.	$\frac{BTU}{lbm°F}$
C_1	Dimensionless constant of correlation by Kurihara and Myers.	———
E	Voltage	volts
F	Variance ratio.	———
h	Boiling heat transfer coefficient.	$BTU/Hr.Ft^{2}°F$
I	Current	amps.
K	Universal constant of simplified Gaertner equation.	———
k_L	Conductivity of liquid.	BTU/Hr.Ft.°F
kT	Average translation energy per molecule.	ergs.
M	Molecular weight of liquid.	gms/gm. mole
N	Number of active sites	———
N_o	Arbitrary constant of Gaertner equation.	———
N^*	Avogardo's constant	1/gm. mole
$\bar{N}$	Average population of active sites on area A.	$sites/ft^2$
n_x	Number of molecular groupings containing x molecules.	———
P_v	Pressure inside bubble nucleus.	$dynes/cm^2$
P_∞	Vapour pressure of liquid.	$dynes/cm^2$
Q	Heat flux.	BTU/hr.

Nomenclature (Continued)

Term	Definition	Units
Q_{LOSS}	Heat loss.	BTU/hr.
R	Gas constant	$\frac{\text{dynes cm}}{\text{gm mole } °K}$
R_o	Radius of critical bubble nucleus.	ft.
R_M	Measured result.	------
S	Nearest neighbor distance between two random adjacent sites.	ft.
T_w	Temperature of the heater surface.	°F
T_B	Temperature of the bulk liquid.	°F
T_{SAT}	Saturation temperature of liquid.	°F
V_o	Bubble volume.	ft^3
V_n	Independent variable.	
V_L	Specific volume of liquid.	ft^3/lbm
W_o	Work required to form bubble of critical size.	ergs.
W_n	Uncertainty in a single variable.	percent
W_R	Uncertainty in a result compounded from several independent variables.	percent
W_x	Activation energy or work necessary to create a cluster of x molecules.	ergs.

Nomenclature (Continued)

Term	Definition	Units
x	Number of molecules.	———
$\beta(R)$	Surface roughness parameter of Kurihara and Meyers equivalent to the number of grooves of size R over a unit area.	———
ε	Characteristic defined by $\frac{4\sigma \tan(\phi/2)}{\rho_L R' T_W}$	———
ρ_L	Density of liquid.	gm/cm^3
σ	Surface tension of liquid.	dynes/cm
Φ	Arbitrary constant of Gaertner equation.	
ϕ	Bubble surface contact angle.	degrees
ρ_o	Density of saturated vapour.	lbm/ft^3
μ_L	Viscosity of saturated liquid.	lbm/ft.hr.

CHAPTER I

INTRODUCTION

Of all the heat transfer processes, boiling has proven to be one of the most complex to analyse. Several theoretical heat transfer models have been proposed for boiling but none are yet capable of correlating existing experimental data.

A prerequisite in the testing of any model is the existence of a comprehensive body of active site density data for various fluid - surface combinations in the nucleate boiling regime*. Heat transfer models have generally been based on the amount of heat transferred to the fluid by a single bubble and in order to evaluate such a model it is necessary to know how many bubbles leave the heated surface in a given length of time. The active site density in combination with the frequency at which bubbles are emitted from a single nucleation site are the two parameters needed to evaluate the total transfer of heat.

One theoretical relationship for predicting the active site density for any fluid - surface combination was proposed by Gaertner[1]. The mathematical expression is stated as

---

* See Appendix A.

$$\frac{N}{A} = N_o \exp\left\{-\left(\frac{16\pi\sigma^3 M^2 N^*}{3\rho_L^2 R^3 [\ln(\frac{P_\infty}{P_v})]^2}\right)\phi(\frac{1}{T_W^3})\right\} \quad (1)$$

where the two constants N_o and ϕ must be evaluated empirically for each set of fluid-surface combinations.

The purpose of the investigation presented in this thesis was to obtain active site density data for five different fluids boiling on a single transparent heater surface with a view to evaluating Gaertner's theory. The transparent heater surface enabled photography of the boiling process from below. A series of still photographs were taken from which the active sites were identified and counted.

In this thesis, literature pertinent to the determination of active site densities is reviewed. A brief discussion of the derivation of Gaertner's site activation theory is also included. Subsequently, the test apparatus, test conditions and test procedures are described in detail. The processes used in the reduction of the photographs to useable data is then presented followed by a summary of the test results. These results are then discussed with regard to their significance. Finally, the conclusions derived from the investigation are presented.

CHAPTER II

LITERATURE SURVEY

The process of nucleate boiling is such that vapour bubbles appear and grow at preferred locations or sites on the heater surface. Early investigators speculated that these special sites were microscopic spines, specks of dirt or oxide, grain boundaries, or tiny pits and scratches. These speculations were invariably accompanied by reports of attempts to count these sites by visual means.

First among these investigations was a report by Jakob and Fritz[2] in 1931. These experimenters observed water boiling at very low heat flux in the nucleate regime and determined a linear relationship between heat flux and the number of active sites. Bubbles rising from the surface presented problems in visually counting the active sites so that site density results were limited to about two active sites per square inch.

In 1955, Corty and Foust[3] made the first detailed study of the effects of surface roughness on nucleate boiling heat transfer. Normal pentane, diethyl ether, and Freon 113 were boiled on copper and nickel surfaces of varying degrees of roughness. Photographs of the boiling process were taken in profile and visual counts of the number of active sites ranging upwards to sixty per square inch for pentane boiling on nickel were reported. In

common with the experience of Jakob and Fritz, bubble congestion above the surface limited the investigation to the low site densities reported.

Theories that the active sites were pits and scratches were presented by Bankoff[4] in 1955, but it was not until 1959 that Clark, Strenge, and Westwater[5] reported experimental evidence as to the correct identity of nucleation sites. Ether and pentane were boiled on a zinc heater surface at low heat flux. A microscope was centered on individual bubbles, after which boiling was stopped and photographs were taken through the microscope of the surface on which the bubble had been nucleating. Analysis of the photographs revealed that pits with diameters between 0.0003 and 0.003 inches were very active nucleation sites. Some scratches and an occasional random speck of foreign material made up the remainder of the sites but in no case did bubbles form at grain boundaries.

In 1960, Kurihara and Myers[6] made the first attempt at predicting the number of active sites for a particular set of boiling conditions. A series of experiments were performed boiling water, acetone, normal hexane, carbon tetrachloride, and carbon disulfide on a copper surface. Using the results obtained, Kurihara and Myers successfully tested an equation which they had derived relating boiling heat transfer coefficients to fluid properties and the number of active nucleation sites. Once

again, the active site count was limited to low heat flux because vision was obscured by the rising bubbles. Their equation for the difference in active site densities between two conditions of superheat incorporates many of the fluid and surface properties included in a later correlation by Gaertner[1]. The equation is stated thusly.*

$$\frac{N_1}{A} - \frac{N_2}{A} = -\frac{C_1}{B}\int_{\Delta T_1}^{\Delta T_2} R^2\ \beta(R)\ \exp\left(\frac{-\varepsilon}{R}\right)\ d(\Delta T) \qquad (2)$$

As can be seen, the equation cannot predict the active site density at a particular set of conditions but can only predict the difference in site density between two different sets of conditions. More elaborate means of counting active sites have since provided data for higher heat fluxes which have proven the equation of Kurihara and Myers to be somewhat in error.

The first attempt at an improved method of counting active nucleation sites was reported by Gaertner and Westwater[7] in 1960. An aqueous solution of nickel salts was boiled on a horizontal flat copper surface in a test cell which contained the boiling activity and enabled electrolytic deposition of a thin film of nickel on the copper surface. The bubble agitation occurring around an active site retarded the plating process and caused a pinhole in the nickel plating. Examination of the surface

---

Kurihara and Myers developed a second equation relating heat transfer coefficients to the number of active sites

$h/K_L = 820\ (\rho_o/\mu_L)^{1/3}\ \bar{N}^{1/3}\ (Pr)^{-0.89}$

after removal from the test cell revealed a random geometrical distribution of pinholes which represented the active sites. Active site densities as high as 1,100 per square inch were obtained.

Following the example of Kurihara and Myers[6], Gaertner statistically analysed the data obtained and reported his findings in Reference (1) in 1963. The spatial distribution of active nucleation site density for boiling water containing dissolved nickel salts was correlated by a Poisson distribution indicating that the active sites were randomly scattered over the surface. In addition Gaertner developed his own expression to predict the active site density for any fluid-surface combination in the nucleate boiling regime. This expression called the Gaertner Site Activation Theory herein has since been tested by additional independent research* which showed the correlation to be in good agreement with all existing empirical data. Because of the importance of Gaertner's expression to the background of the current investigation, the derivation is presented in Chapter III of this thesis.

At approximately the same time that Gaertner presented his relationship, Kirby and Westwater[8] developed a much improved method of counting active nucleation sites.

---

* See the work of Judd[10].

The apparatus which they employed utilized a transparent heater surface which enabled photography of the boiling action occurring on the flat horizontal surface from below. Carbon tetrachloride and methanol were boiled and high speed motion pictures were taken. From the pictures, bubbles were traced to their nucleation sites and site densities ranging from 330 to 4,050 sites per square inch were successfully determined.

Gaertner[9] published additional data for water boiling on a flat horizontal copper surface in 1965. The active site densities were evaluated by visual count from a profile view of the boiling and were only a byproduct of the total investigation which centered more on bubble interaction above the boiling surface.

In 1968, Judd[10] reported further experimentation using the transparent heater technique. Judd tested the Gaertner Site Activation Theory with data obtained from boiling Freon 113 on the transparent glass heater surface. In addition Judd demonstrated that the data of Kirby and Westwater[8] also correlated well and in deriving the arbitrary constants of the expression (N_o and Φ) he observed that the lines through his data, that of Kirby and Westwater, and that of Gaertner appeared nearly parallel. This observation implied that the Gaertner expression might be somewhat

simplified* but at that time sufficient data was not available to test the hypothesis.

---

* The simplification is presented as Equation (21).

CHAPTER III

DERIVATION OF THE GAERTNER SITE ACTIVATION THEORY

The derivation presented in this chapter is based upon the derivation outlined in Reference (1). Analytical studies of nucleate boiling based on hydrodynamic interactions and local heat flow at the surface which preceeded the work of Gaertner were characterized by the assumption that active sites were distributed in some regular geometric pattern such as a square array. Gaertner statistically analysed active site density data drawn from Reference (7) and found that it fitted a spatial distribution described by the Poisson equation.

$$P_u(x) = \frac{e^{-u}U^x}{x!}$$

where $P_u(x)$ is the probability that event x will occur when the mean or expected value of x is U. The Poisson distribution arises if a large number of discrete events occur randomly over a long period of time or over a large area with the random variable being the frequency with which these events will occur in any small time or small area chosen at random. This spatial orientation negated any assumption that the active sites are ordered or even clustered as is seemingly apparent in nucleate boiling. Gaertner terms this illusion "a visual manifestation of a completely random distribution".

Having offered proof that the active sites were

randomly distributed over the heater surface, it was possible for Gaertner to use an equation derived by Clark and Evans[11] for the two-dimensional distribution of nearest-neighbor distances. Considering a random array of sites, if an arbitarily selected site A_1 is chosen as a reference point, the approximate distance to the nearest neighbor A_2 is represented by a circle whose center is A_1 and whose radius is S. The probability that no active site will be found in the circle is given by the Poisson equation

$$P = e^{-\bar{N}\pi S^2} \tag{2}$$

and the probability that only one active site A_2 will be found in a shell of area $2\pi SdS$ is

$$P = \bar{N}2\pi SdS \tag{3}$$

Multiplying equations (2) and (3) gives the probability that A_2 is the nearest neighbor of A_1 thus

$$P(S < S < S + dS) = 2\pi\bar{N}Se^{-\bar{N}\pi S^2}dS \tag{4}$$

Using site density data drawn from Reference (7) as a check, Gaertner was able to determine the average nearest neighbor distance to be represented by the expression

$$\bar{S} = 1/2\ \bar{N}^{1/2} \tag{5}$$

Gaertner assumed that the spatial distribution defined by this equation was dependent on the liquid-surface properties, system pressure, and the surface temperature and set about developing a correlation which predicted active site densities

in agreement with the distributions described by Equation (5). The argument went as follows.

Statistical thermodynamics predicts that the number of molecular groupings capable of spontaneously forming a nucleus in a fluid of infinite extent is represented by

$$n_x \alpha \exp \left(- \frac{W_x}{kT} \right) \tag{6}$$

where

n_x is the number of molecular groupings containing x molecules.

W_x is the activation energy or the work necessary to create a cluster containing x molecules.

kT is the average translation energy per molecule.

The term W_x may be considered as the work required to form a "hole" in the liquid by shoving it back and creating an interfacial surface between liquid and vapour.

Assuming spherical clusters having radius R_o, volume V_o, and surface area A_o, then

$$W_x = -V_o \Delta P + \sigma A_o \tag{7}$$

where $V_o \Delta P$ is the pressure volume work and σA_o is the surface area work. Now for a spherical bubble, it can be shown that

$$V_o \Delta P = V_o (P_v - P_\infty) = \frac{4}{3} \pi R_o^3 \left(\frac{2\sigma}{R_o}\right) = \frac{8}{3} \pi R_o^2 \sigma \tag{8}$$

and

$$\sigma A_o = 4\pi R_o^2 \sigma \tag{9}$$

Substituting Equation (8) and Equation (9) in Equation (7)

$$W_x = -\frac{8}{3}\pi R_o^2\sigma + 4\pi R_o^2\sigma = \frac{4}{3}\pi R_o^2\sigma \tag{10}$$

Also for a spherical bubble it can be shown that

$$P_v - P_\infty = \frac{2\sigma}{R_o} \tag{11}$$

Substituting Equation (11) in Equation (10) yields

$$W_x = \frac{16\pi\sigma^3}{3(P_v - P_\infty)^2} \tag{12}$$

Now Poynting's equation for a perfect gas states that

$$V_L (P_v - P_\infty) = kT \ln \left(\frac{P_\infty}{P_v}\right) \tag{13}$$

where V_L is the volume of one molecule of liquid given by $V_L = \frac{M}{\rho_L N^*}$ and k is Boltzman's constant represented by $k = R/N^*$.

Furthermore, T can be considered to be T_W where T_W is the wall temperature. Substituting for V_L, k, and T_W in Equation (13) results in

$$\frac{M}{\rho_L N^*} (P_v - P_\infty) = \frac{R}{N^*} T_W \ln \left(\frac{P_\infty}{P_v}\right) \tag{14}$$

Substituting Equation (13) in Equation (12)

$$W_x \approx \frac{16\pi\sigma^3 V_L^2}{3\left[kT \ln \left(\frac{P_\infty}{P_v}\right)\right]^2} \tag{15}$$

Temporarily assuming nucleation to be homogeneous, Gaertner combined Equation (15) with an absolute rate equation having a space dimension of surface area to obtain an equation for the active site density. The resulting expression is

$$\frac{N}{A} \alpha \exp -\left\{ \frac{16\pi\sigma^3 M^2 N^*}{3\rho_L^2 R^3 [\ln(\frac{P_\infty}{P_v})]^2} \left(\frac{1}{T_W} \right)^3 \right\} \tag{16}$$

Gaertner introduced two arbitrary constants N_o and Φ into this relationship to modify it for heterogeneous nucleation on a heat transfer surface. The final equation obtained is

$$\frac{N}{A} = N_o \exp\left\{ - \left(\frac{16\pi\sigma^3 M^2 N^*}{3\rho_L^2 R^3 [\ln(\frac{P_\infty}{P_v})]^2} \right) \Phi \left(\frac{1}{T_W} \right)^3 \right\} \tag{17}$$

In 1962, Hsu[12] presented a theory for the size range of active nucleation sites based on thermodynamic and heat transfer considerations. In the analysis, equations were provided for the size range of cavities acting as active sites and the criterion for the incipience of boiling was established. This theory predicts the necessary condition for nucleate boiling to occur but cannot supply the sufficient condition. Gaertner's theory may be considered to predict the sufficient condition fullfilling Hsu's theory. Gaertner's relationship is incomplete as a prediction however in as

much as there is no theoretical means of evaluating the two arbitrary constants N_o and ϕ and consequently these constants still have to be found experimentally.

CHAPTER IV

EXPERIMENTAL APPARATUS

A. Introduction

No previous research in boiling heat transfer had been conducted at McMaster University and as a consequence it was necessary to design and construct all of the primary equipment utilized in the investigation. It was essential that the apparatus be capable of the following functions.

1. Maintaining the test fluid at saturation temperature throughout the experiment.
2. Containing pressures within the test cell ranging from atmospheric to 70 pounds per square inch.*
3. Supporting a transparent flat horizontal heater surface in such a position that boiling taking place on the surface could be photographed from below.
4. Supplying continuous D.C. power to the transparent conductive oxide coating on the glass test surface in order to sustain boiling.
5. Directing intense back lighting through the fluid to the heater surface to illuminate bubbles adjacent to it.

---

* In this investigation, data for atmospheric and 8 pounds per square inch only was collected. However the test cell was tested as high as 40 pounds per square inch without failure occuring.

6. Detecting and measuring temperatures in the liquid and at the heater surface.

The apparatus was designed to incorporate an existing transparent heater surface design which is described in Reference (10). Five liquids, Freon 113, carbon tetrachloride, chloroform, dichloroethane, and trichloroethane, were tested. The choice of test fluids was limited to those with relatively low boiling points* for which gasket materials used in the test cell were inert. Further details of the design and operation of the apparatus are presented in the sections which follow.

B. Heater Surface

The transparency of the heater surface was the most important feature of the apparatus in as much as it permitted photography of the boiling occurring on the upper surface from below. The design is essentially the same as that used by Judd[10] and is also very similar to that employed by Kirby and Westwater[8]. The heater surface is shown in Figure (1).

The surface was placed horizontally in a depression in the bottom of the test cell. Three such test surfaces were used in the course of the experiment. The first surface

---

* The fluid with the highest boiling point tested was trichloroethane (B.P. 239°F).

was used to boil Freon 113 and carbon tetrachloride but was inadvertently destroyed while an attempt was being made to boil glycol as the third test fluid. For reasons unknown, glycol reacted with the oxide coating on the heater surface and its conductivity and transparency deteriorated in a matter of minutes. A second surface, identical to the first was used for the remaining tests including a retest of Freon 113 to check the repeatability of the data obtained from the first surface. A third surface, an original of the type used by Judd[10] and differing from the other two only in that the thickness of the glass was one eighth inch instead of five millimeters, was used in the final test with the cell pressurized to check the results reported in Reference (10).

Fourteen heaters were prepared according to the specifications shown on Figure (1) by Corning Glass Works. As noted in Reference (10), the variation in electrical resistance of the oxide coating was considerably less than one ohm among the sample of fourteen heaters. In addition, no measureable change in resistance took place during the course of the experiment with the exception of the failure encountered during the glycol test.

A chromel-constantan thermocouple was epoxyed to the bottom of the heater surface for the purpose of measuring its temperature. The unit was then placed in the prepared depression and clamped down against a rubber gasket to prevent

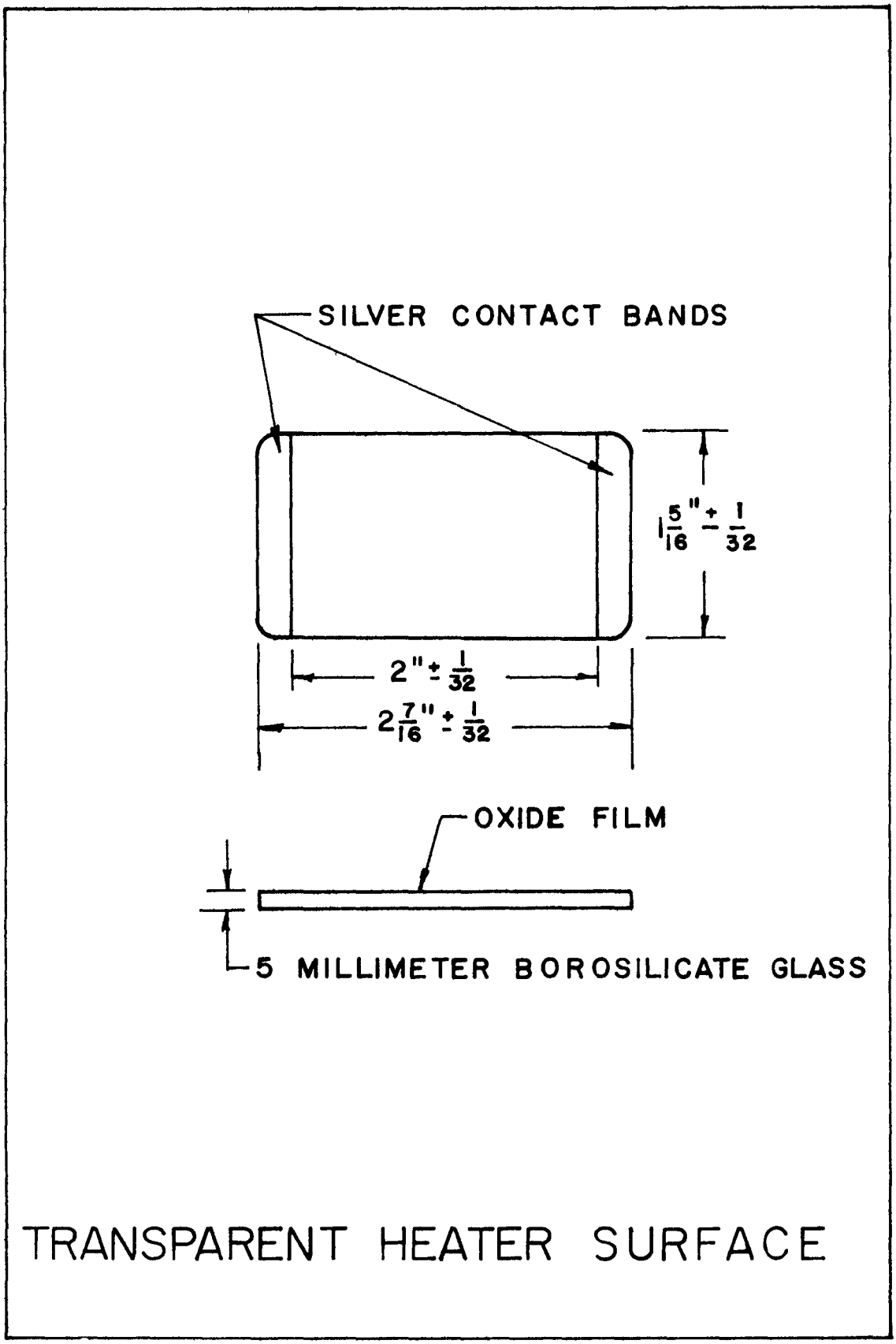

FIGURE 1. DRAWING OF TRANSPARENT HEATER SURFACE

leakage of the test fluid.

C. Test Cell

Three main criteria were considered in the design of the test cell.

1. It must contain the test liquid and be compatible with it at the saturation temperature of the liquid.
2. It must facilitate photography of the bubbles nucleating on the transparent heater surface.
3. The design must be easily disassembled for thorough cleaning and change of test fluid.

Of the three criteria, number one proved later to be the hardest to fulfil, and some test fluids had to be rejected and substitutes used. The photographic parameters were well met and after initial adjustments, photography of the bubbles was accomplished with no difficulty. Trouble with back lighting which had been anticipated never arose and it was possible to photograph the boiling over a wide range of heat flux. Disassembly presented no problems and after minor modifications resulting from experience gained in initial testing had been made, total time for complete cleaning operations and change of fluid was of the order of about two hours.

Figure (2) is a detailed drawing of the assembled test cell shown in Figure (3) and Figure (4). The cylindrical wall of the container was constructed from 6 inch, schedule

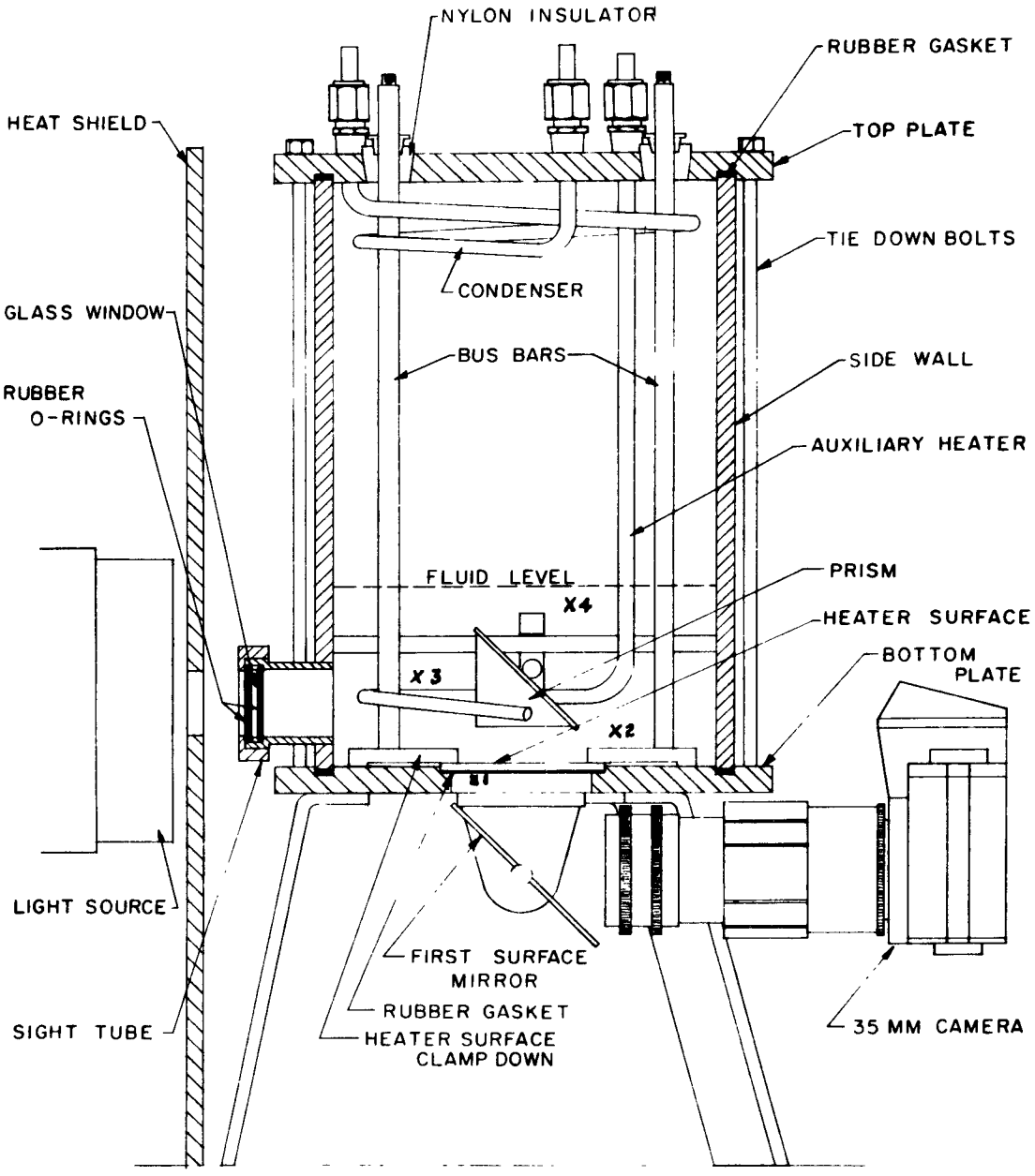

FIGURE 2. DETAILED DRAWING OF TEST CELL

40, type 304 stainless steel pipe. The top and bottom were machined from 1/2 inch thick type 304 stainless steel plate. The top, bottom, and side wall were held together by six 1/4 inch diameter tie down bolts spaced around the outer periphery of the cell. The joints between the top, bottom, and side wall were sealed using Buna-N rubber gaskets recessed in circular grooves in the top and bottom plates.

The transparent heater surface was mounted horizontally in a depression in the bottom of the cell. Two type 304 stainless steel clamps held the surface firmly in place compressing a Buna-N rubber gasket which provided a leak-proof seal. The clamps which were electrically insulated from the bottom of the cell made contact with the silver contact bands of the test surface. Two type 304 stainless steel tubular bus bars transmitted D.C. power from the power supply through the top of the test cell and down to the hold down clamps.

Fluid level in the test cell was maintained five inches above the test surface throughout the investigation. The fluid was kept at saturation temperature by an auxiliary 1/4 inch diameter, 115 volts, 100 watt tubular heater. A.C. power to this heater was controlled by a 1.4 KVA Variac. A 1/4 inch diameter type 304 stainless steel condenser coil with a condensing area of approximately 30 square inches was located in the upper part of the test cell to condense vapour thus maintaining saturation conditions in the cell.

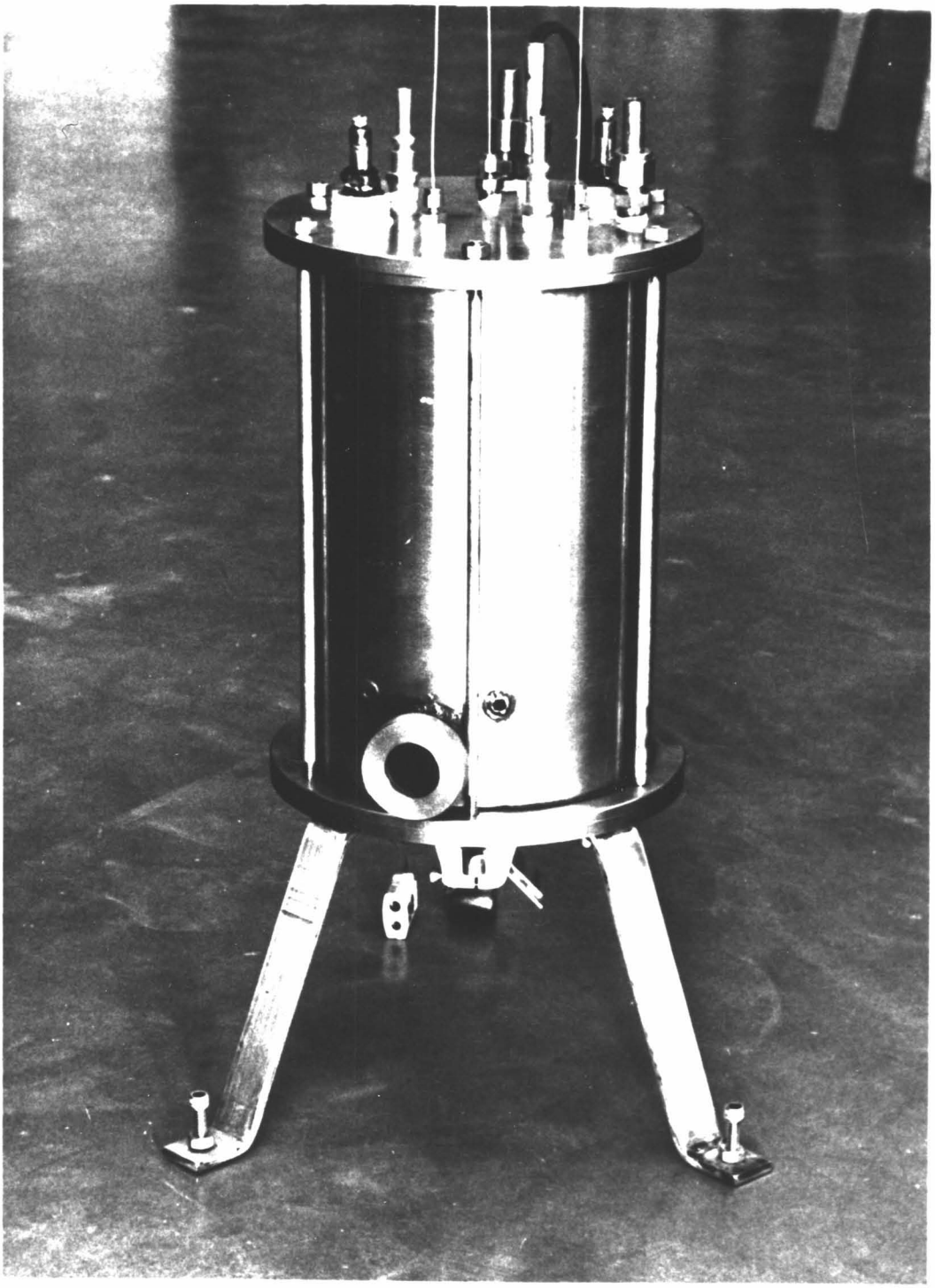

FIGURE 3. PHOTOGRAPH OF TEST CELL

A sight tube machined from type 304 stainless steel bar stock was welded to the side wall of the cell about one inch above the bottom. It contained a 1.142 inch diameter by .118 inch thick optically flat glass disc sealed in place with two Buna-N rubber "O" - rings which provided a window through which an intense beam of light could be directed into the test cell. The light beam was deflected ninety degrees by a silvered prism through the transparent heater surface and onto a flat first surface mirror which again deflected the beam ninety degrees into the lens of the camera. Both the mirror and prism mounts allowed movement in two directions while rotation of the side wall of the test cell provided the third degree of freedom for sighting in the equipment.

The test cell was supported on three legs made from 1/4 inch thick type 304 stainless steel plate. The legs were provided with leveling screws for leveling the system.

D. Thermocouples

Four thermocouples were used in the experiment, all of which were made of chromel-constantan because of the high EMF characteristics of this combination in the temperature range studied. As described in the section on the heater surface, a thermocouple was fastened to the lower surface of the glass plate using Lepage's epoxy . This thermocouple which measured the temperature of the heater

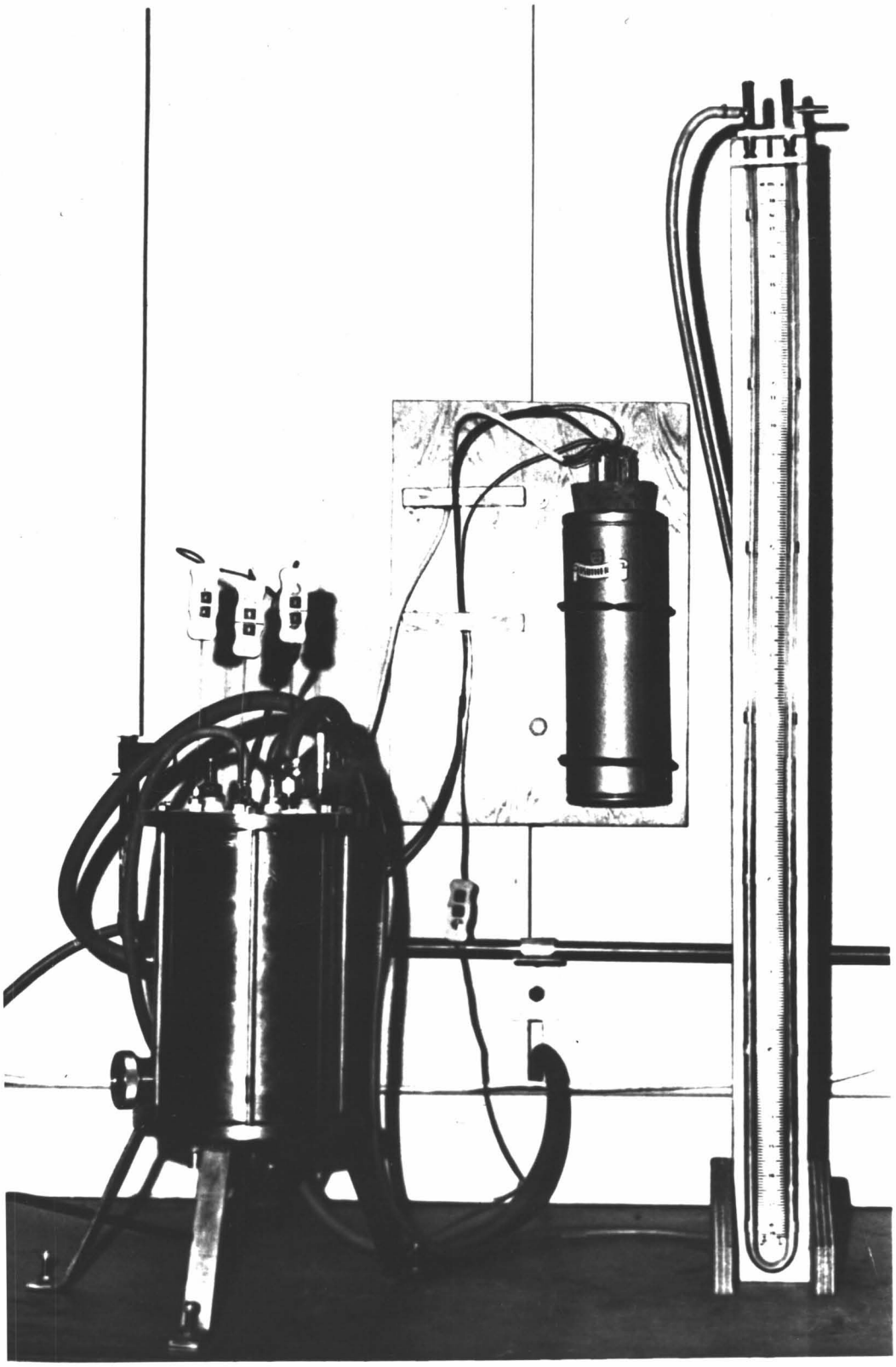

FIGURE 4. PHOTOGRAPH OF TEST CELL AND SUPPORTING EQUIPMENT

surface was designated number one. It was constructed from 36 gauge vinyl coated wire.

Thermocouples two, three, and four were located 1/2 inch, 1 inch, and 2 inches above the bottom of the test cell respectively to record temperature deviations in the bulk liquid. These thermocouples were supplied as complete assemblies by Thermoelectric Company and were designated by them as probe type 5E0110L Ceramo with ungrounded hot junctions.

The positions of the four thermocouples are marked by numbered x's on Figure (2). Connector plugs allowed easy disconnection of the thermocouples during disassembly of the apparatus for cleaning. The transition to copper lead wires was made in oil filled glass tubes submerged in an ice bath. Switching between thermocouples was accomplished by double pole double throw copper knife switches.

The output of the thermocouples was measured with a Guildline photocell galvanometer potentiometer, model 9160-G shown in Figure (5). This instrument was capable of measurement accurate to 10^{-6} volts. All three probe type thermocouples consistently gave readings within two tenths of a degree of one another at the saturation temperature of the test fluid. Prior to the beginning of the experiment, the thermocouples had been tested in an ice bath and gave essentially identical readings within 2 μ volts of the null.

FIGURE 5. PHOTOCELL GALVINOMETER POTENTIOMETER

E. Photography

The usefulness of the experimental data was entirely dependent on the successful photographing of the active nucleation sites on the heater surface. The means by which photography of the surface from below was accomplished has already been discussed in the section describing the test cell. The most important and hardest to predict parameter in the success of the photographic experiment was back lighting. As the heat flux was increased, the larger number of bubbles rising from the surface tended to diffuse the incoming beam of light. This problem of shading was overcome by using a 750 watt photo flood lamp as a light source. This light source provided sufficient back lighting up to and beyond heat fluxes for which the active sites density could be determined by still photography.

A much more critical lighting problem was encountered at low heat flux, where an insufficiency of bubbles rising from the surface left gaps in the background through which light passed unobscured. This phenomenon tended to "wash out" definition of the few existing bubbles at this heat flux and considerable experimentation had to be done to find exposure settings which would make the bubbles visible. Developing and printing techniques which improved with experience over the course of the experiment assisted in improving the pictures at low heat flux.

Also of concern at low heat flux was the heat input from the photo flood lamp. First order approximations based on the difference in light meter readings taken ahead of the test cell and after the beam had passed through the fluid indicated that at low heat flux the light source could account for as much as twenty-five percent of the total heat input. To minimize this effect, a 1/4 inch thick type 304 stainless steel shield was placed between the light source and the test cell as shown in Figure (2). A 1 inch diameter hole provided an aperture for the light beam and shielded the remainder of the cell. Tests conducted with and without the shield in place indicated that heat loads were substantially reduced by using the shield. It is estimated that at no time during data taking was the light accounting for more than five percent of the heat input and although the temperature of the heater surface was continually monitored, no measureable change was ever observed when the light was switched on or off. To further minimize the heating effect, photographs were taken in intermittent groups with pauses during which the light was turned off.

Photography was accomplished using a Practika 35 millimeter camera fitted with an Asahi Tachumar close up lens. Although the lens could be focused from infinity to a focal length of seven inches, all photographs of the boiling were taken at a focal length setting of 8.25 inches. Depth

of field tests* conducted at this setting indicated a depth of field at the 8.25 inch focal length of approximately .040 inches. This feature was desirable in as much as it assured that the bubbles which appeared in the photographs either were still attached to the heater surface or were located immediately above it. Assurance that the bubbles in the photographs were very close to or on the heater surface produced a high degree of confidence that a count of the bubbles closely paralleled a count of the active nucleation sites.

Film used throughout the experiment was Kodak Tri-X. Shutter speed was constant at 1/500 seconds and the F-stop on the lens aperture was varied to adjust for lighting conditions.

F. Power System

Figure (6) and (7) are photographs of the power supply used in the investigation. A bank of 14 twelve volt wet cells provided D.C. power from zero to 168 volts open circuit. Capacity of the system was 5 amps. The battery system was chosen over a rectifier because the cost of a rectifier combining sufficient capacity and very low ripple far outweighed the inconvenience of recharging the batteries. The batteries were wired through knife switches which allowed

---

* See Appendix C.

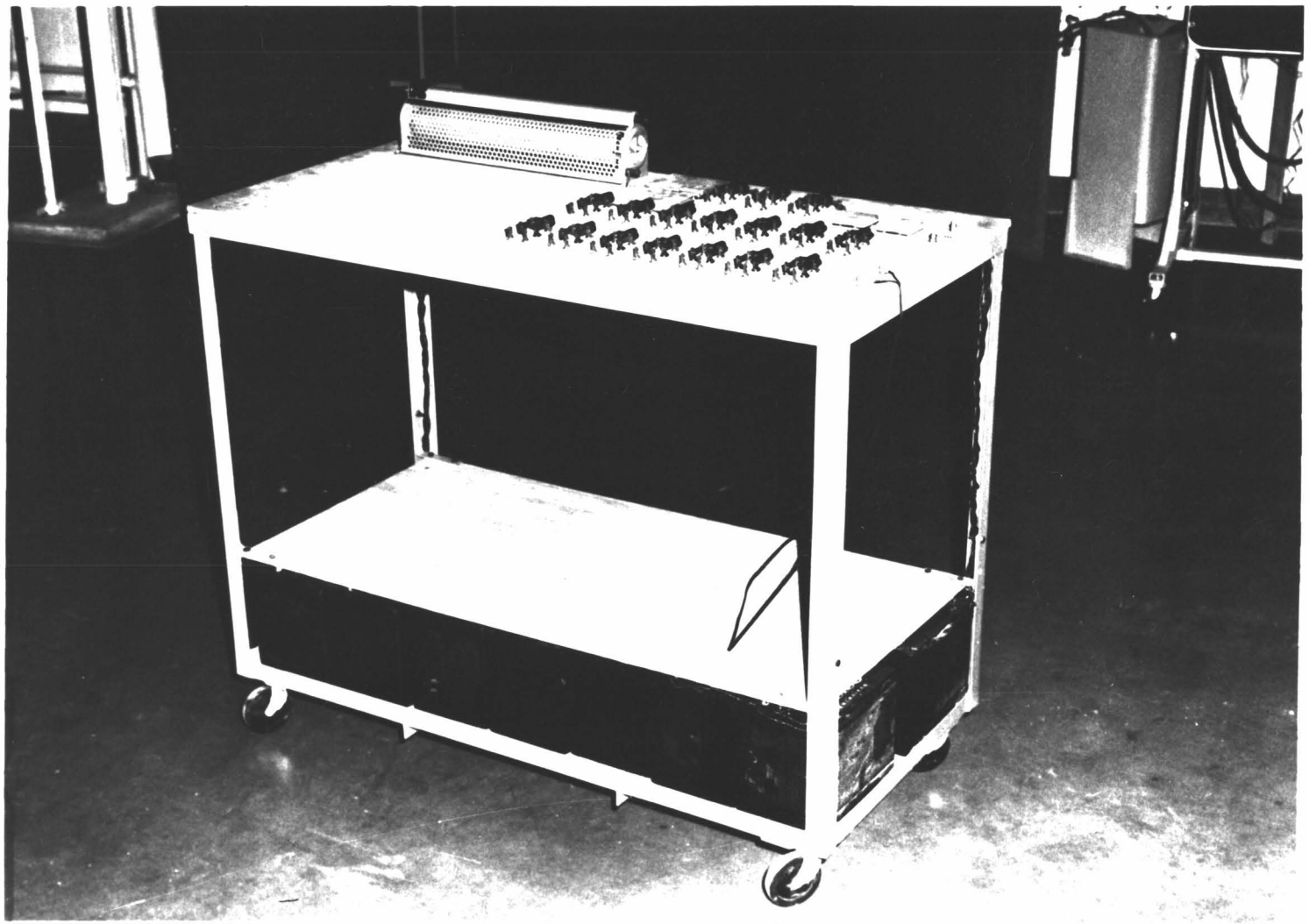

FIGURE 6. D.C. POWER SYSTEM

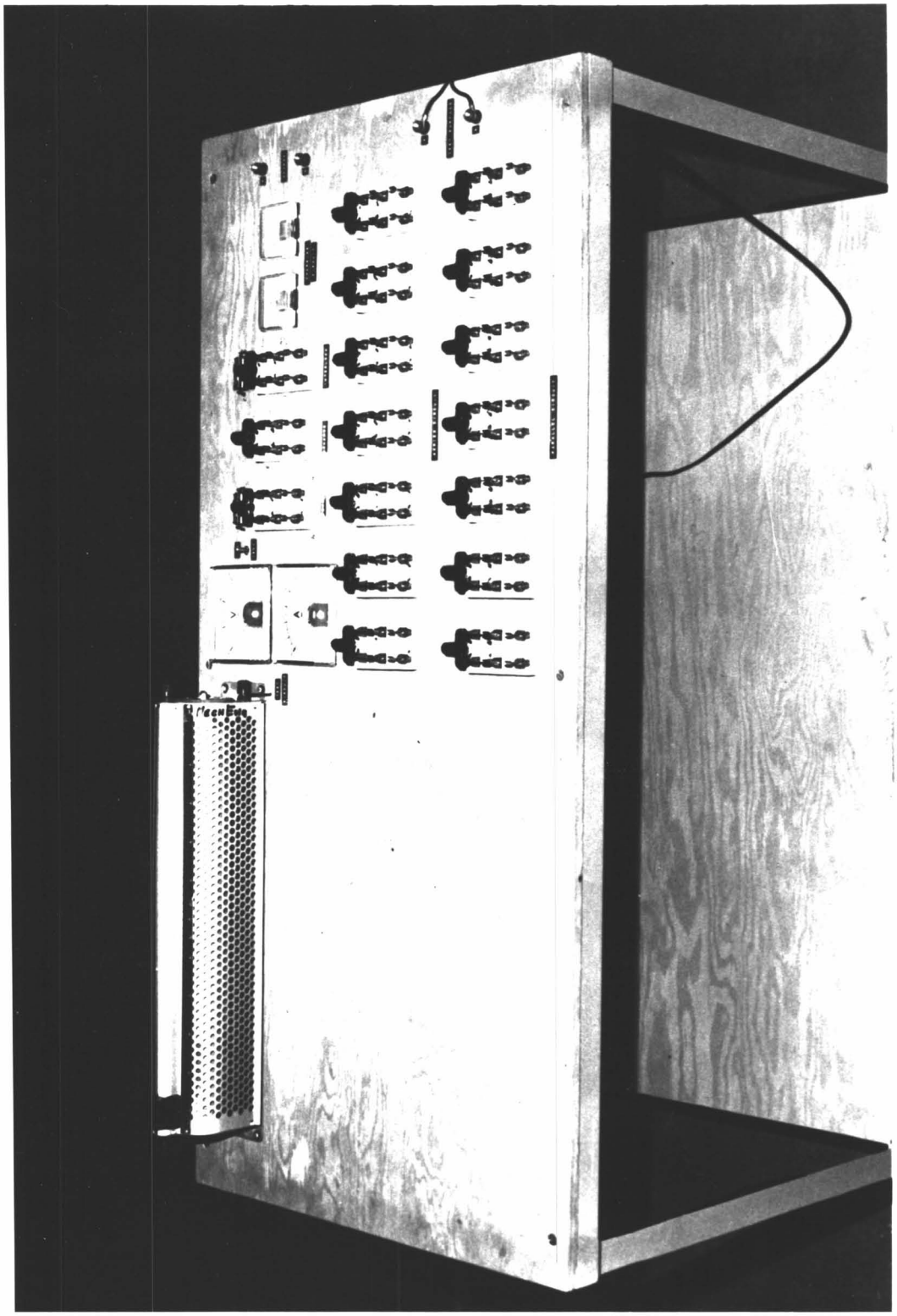

FIGURE 7. CONTROL PANEL OF POWER SYSTEM

each battery to be connected either in parallel with the rest for recharging or with any number of the others in series to supply a required voltage. A slide wire resistor in series with the batteries supplied an infinite range of voltage settings between the 12 volts increments of the batteries.

A calibration test of the ammeter and voltmeter in the output from the power system using known fixed resistances produced the calibration curve* shown in Figure (8). Meter error was in the order of 4 percent at the upper end of the operating range.

G. Pressurization System

With the exception of one test series, this experiment was conducted at atmospheric pressure. However, the ability to pressurize the system was a desirable feature for future investigations. For the one test series requiring pressurization, a pressure of 8 pounds per square inch gauge was achieved without difficulty using a helium atmosphere. Helium was used to reproduce the test conditions reported in Reference (10). Other gases could have been used equally well with the equipment.

The cylinder pressure in the helium bottle of 2300 pounds per square inch gauge was regulated from zero to 40 pounds per square inch in the test cell by a diaphram

---

* See also Appendix B.

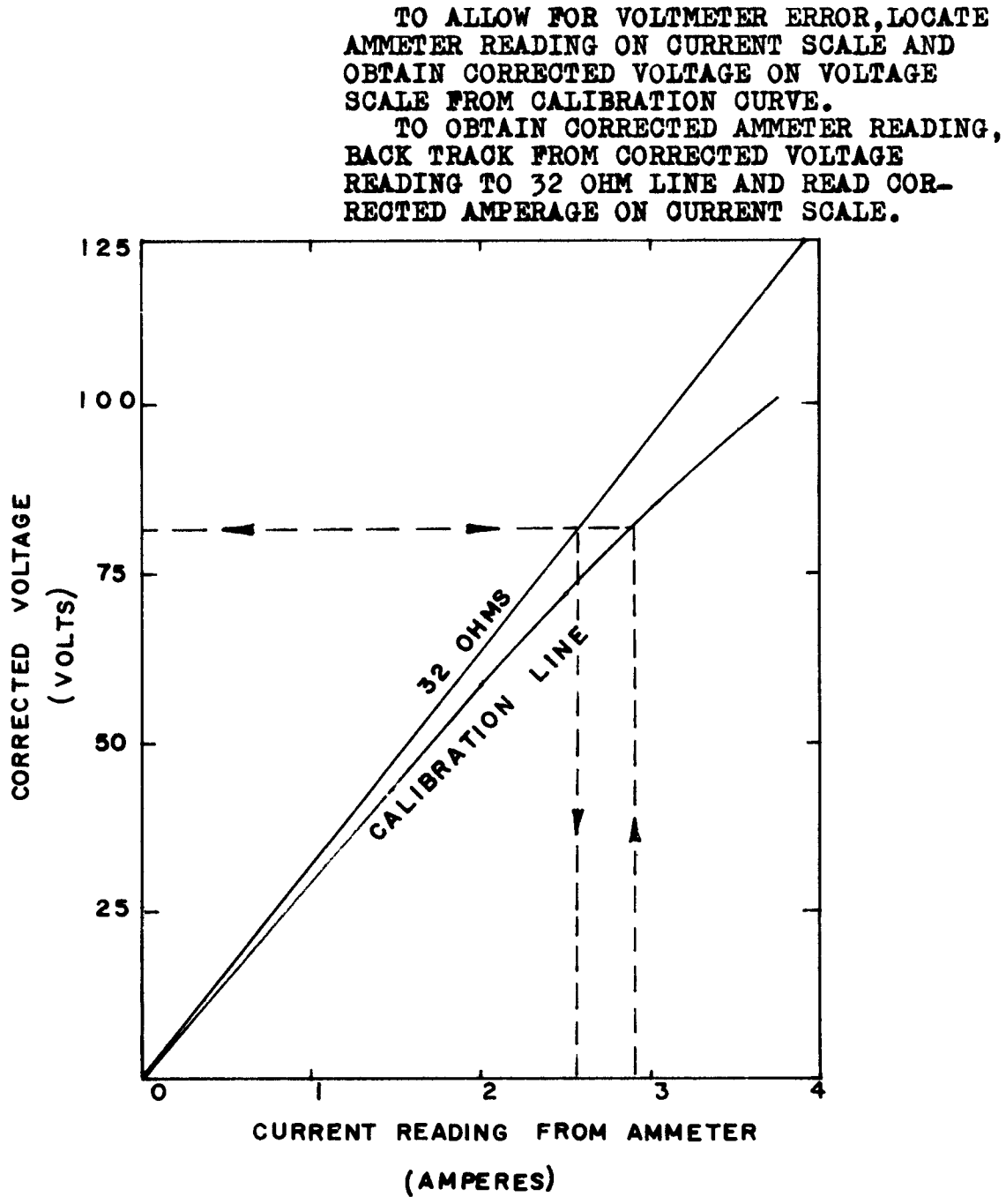

FIGURE 8. CALIBRATION CURVE FOR METERS ON POWER SYSTEM

regulator. Tests of the equipment were conducted up to 40 pounds per square inch gauge without failure. Pressure in the test cell was measured using a mercury filled U-tube manometer.

CHAPTER V

TEST CONDITIONS

Five fluids, Freon 113, carbon tetrachloride, chloroform, dichlorethane, and trichloroethane were tested. Reasons for the selection of these particular fluids are several. Primarily all have relatively low boiling points ranging from Freon 113 (B.P. 117.2°F) to trichloroethane (B.P. 239°F) at atmospheric pressure.

Originally, it had been planned to test at least one fluid having a much higher surface tension such as silicon oil. Unfortunately it was discovered that the fluids with higher surface tensions tend to have much higher boiling points of the order of 400°F to 500°F and this far exceeded the capabilities of the equipment. The five fluids selected represent as wide spread a range of surface tension as is obtainable from the lower boiling point fluids. Freon 113 has the lowest surface tension of the fluids tested of 19.6 dynes per centimeter while trichloroethane is highest at 33.6 dynes per centimeter, both evaluated at 68°F.

Freon 113 was chosen as the first fluid to be tested because Reference (10) had shown it to be very compatible with the transparent heater surface and the data reported served as a check on the site counting by still photography technique which was proposed for the current investigation.

The low boiling point of Freon 113 did not strain the as yet untested equipment and the high active site densities which are characteristic of this fluid* served as a good check of the counting technique. The active site densities for Freon 113 were anticipated to be the highest that would be experienced in the course of the investigation and if these densities could be accurately determined it was reasonable to assume that the other fluids would present no problems.

Carbon tetrachloride was chosen as the second fluid because existing data reported by Kirby and Westwater[8] served as a check. Glycol was to be the third fluid because of its higher surface tension. However long before saturation temperature was reached, the glycol reacted with the oxide coating on the heater surface and rapid deterioration of both its conductivity and transparency resulted.

Methanol was chosen as a substitute for glycol because Kirby and Westwater[8] had reported its use in their equipment. It is interesting to note however that only site density data for carbon-tetrachloride was published. In the current investigation, it was found that methanol had much the same effect as glycol, destroying the heater surface in

---

* The low specific heat of Freon reduces the amount of heat which can be transferred to the bulk liquid by natural convection and hence boiling occurs readily and increases rapidly with increased heat flux.

a matter of minutes. In view of observations reported by Judd[10] and by Kirby and Westwater[8] as to the electrolytic reaction occuring between the oxide coating and boiling water, it is reasonable to speculate that even small amounts of water such as might be present in methanol and glycol by virtue of their mutual solubilities have much the same effect.

The next fluid tested for compatibility with the equipment was chloroform. No deterioration of the oxide coating on the heater surface was apparent but prolonged contact with the rubber gaskets in the test cell did cause swelling and eventual shreading of the rubber and resulted in a yellow discoloration of the fluid. The same discoloration was noticed to a lesser extent with Freon 113 and carbon tetrachloride but only after periods of several days. In all tests, data taking was completed within two hours after the test cell had been charged with fresh fluid. This procedure was felt sufficient to rule out the possibility of contamination of the fluid by the rubber.

The compatibility of carbon-tetrachloride and chloroform provided a strong argument for remaining in the Chlorinated Hydrocarbon family for other test fluid selections. Dichloroethane and trichloroethane were the next two selected and both fluids proved compatible with the oxide surface. Again, eventual deterioration of the rubber gaskets had to be guarded against. The higher boiling point of these last two fluids

TABLE 1

SUMMARY OF TEST CONDITIONS

TEST SER.	TEST POINT	FLUID	$\frac{Q}{A}$	INTERNAL PRESSURE	GLASS PLATE	REMARKS
#	#		$\frac{BTU}{HR.FT.^2}$	PSIG.	#	
1	1	FREON113	5124	ATMOS.	1	
"	2	"	7466	"	"	
"	3	"	12078	"	"	
"	4	"	16333	"	"	
"	5	"	21228	"	"	
2	1	CCl_4	5124	ATMOS.	1	
"	2	"	8230	"	"	
"	3	"	12078	"	"	
"	4	"	16333	"	"	
"	5	"	21228	"	"	
3	1	CHLORO-FORM	4949	ATMOS.	2	
"	2	"	7780	"	"	
"	3	"	11280	"	"	
"	4	"	15390	"	"	
"	5	"	20150	"	"	
4	1	FREON113	7466	ATMOS.	2	REPRODUCIBILITY TEST OF SECOND SURFACE.
5	1	DICHLORO ETHANE	4949	ATMOS.	2	
"	2	"	7780	"	"	
"	3	"	11280	"	"	
"	4	"	15390	"	"	
"	5	"	20150	"	"	
6	1	TRICHLORO ETHANE	4949	ATMOS.	2	
"	2	"	7780	"	"	
"	3	"	11280	"	"	
"	4	"	15390	"	"	
"	5	"	20150	"	"	
7	1	FREON113	5124	8PSIG.	3	REPRODUCIBILITY TEST OF JUDD'S DATA FOR FREON BOILING UNDER PRESSURE.
"	2	"	8235	"	"	
"	3	"	11803	"	"	
"	4	"	16333	"	"	
"	5	"	20862	"	"	

was a desireable feature in obtaining data for as wide a spread of fluid conditions as possible.

Table (1) is a summary of the tests conducted. Seven series of tests were performed, each series having five heat flux settings except for Series 4 which was a reproducibility test of Freon 113 at a single heat flux setting. All test series were conducted at the saturation temperature of the test fluid and with the exception of Series 7, all tests were performed at atmospheric pressure.

Heat flux settings ranged in each test series from approximately 5,000 BTU per hour square foot to about 20,000 BTU per hour square foot. The incipience of boiling for each fluid tested varied slightly but in all cases was very near a heat flux setting of 5,000 BTU per hour square foot. The upper limit of heat flux for each test series was fixed at the point at which horizontal coalescence of the bubbles made the counting of individual active sites by still photography impossible. In the case of all fluids this condition was achieved at approximately 20,000 BTU per hour square foot with the lower boiling point fluids approaching this condition at slightly lower values of heat flux.

CHAPTER VI

TEST PROCEDURE

A series of equipment tests were performed prior to the commencement of actual data taking in order to perfect photographic techniques. These tests consisted of the following.

1. A test of the close up lens to explore the range of aperture settings for various heat fluxes.
2. A series of depth of field tests* performed at a focal length of 8.25 inches which had been found to be the setting required when the camera was focused on the heater surface.
3. A lens focusing test with the reference grid in place to determine the best overall definition of grid and bubbles over the range of heat fluxes.
4. A lighting test to determine optimum lighting conditions at various heat flux settings.
5. Two preliminary test runs of the complete system during which bubble photographs were taken to provide data to check the still photography technique for counting active sites. The data obtained from the two test

---

* See Appendix C.

runs, one at low heat flux and one at high, was used to test a computer program which was devised to correlate the active sites observed in the twenty still photographs taken during each of the test runs.

The test fluid used for all of the initial equipment tests was Freon 113. Atmospheric pressure was maintained in the test cell and saturated boiling conditions were established.

As stated in Chapter V, five different test fluids were investigated during the course of the experiment. The investigation was comprised of seven test series all of which were conducted at saturated boiling conditions. With the exception of Test Series 7, all tests were performed at atmospheric pressure. As expected, the time required to reach steady state operating conditions from a cold start varied with the thermophysical properties of the test fluid. This time ranged from approximately 25 minutes for Freon 113 to about 45 minutes for trichloroethane.

During the warm-up period, thermocouples in the bulk liquid recorded temperature deviations in the fluid of the order of 5°F. As the saturation temperature was approached, these deviations lessened and at saturation temperature all three thermocouples gave readings within two-tenths of a degree of each other and of the reported saturation

temperature of the test fluid. The apparatus was considered to be at steady state operating conditions when the three thermocouples in the bulk liquid and the single thermocouple on the underside of the heater surface gave readings which varied by less than 1/10°F in a five minute period.

Prior to an actual test run, an equipment test was made using the proposed test fluid to check the range of the heat flux settings to be used in the test. A discussion of the criteria used in choosing the heat flux range is given in Chapter V. After the preliminary test was completed, the test cell was drained and refilled with fresh fluid and data taking was performed as soon as the system regained saturation conditions to guard against possible contamination of the test fluid by the rubber gaskets in the test cell.

A typical test sequence proceeded as follows.

1. When invariant temperature readings from the four thermocouples were obtained, the readings were recorded.
2. The light source was switched on and exposure meter readings were taken to establish lens aperature settings. If the heat flux was low, a visual count of the active sites was performed for comparison with the count obtained from the photographs.

3. The light source was switched off and the thermocouple readings were checked.
4. The light was switched on and the first ten exposures were taken.
5. The light was switched off for a five minute period during which time the heater surface temperature was monitored to check for changes which might have resulted from heat input from the lamp. However this effect was never observed in any of the test series.
6. The light was switched on again and the last ten exposures were taken.
7. The thermocouple readings were checked once more.

The addition of a helium atmosphere to pressurize the test cell for the last test series did not change the test sequence. Pressurization took place at the time when the equipment was turned on to warm up and was continued throughout the entire test.

CHAPTER VII

DATA REDUCTION

A. Introduction

In this chapter, the methods by which the raw data was transformed into useable information is explained. Millivolt readings from the three thermocouples in the bulk liquid and the single thermocouple attached to the heater surface were recorded and converted into temperature readings using temperature-millivolt conversion tables for chromel-constantan thermocouples. The barometric pressure and the room temperature were recorded and the power input to the heater surface was computed from the measurements of the voltmeter and ammeter in the power supply. These readings were corrected for meter error using the calibration chart prepared for the power system and shown in Figure (8).

The active site density data was recorded in the form of photographic prints of the boiling occurring on the transparent heater surface taken from below. Photographic techniques are discussed in Chapter IV. Twenty still close-up photographs were taken at random time intervals for each test run at a particular heat flux setting. The processes by which the photographs were interpretted to produce useful active site density data is examined in detail below.

The remainder of the chapter is comprised of four parts. Firstly a discussion is presented on how the sets of twenty photographs were analysed to identify active sites. Secondly, the use of a digital computer for counting the sites identified on the photographic prints is discussed and justification of this counting technique and its accuracy is presented. Following this, a section is devoted to the analysis of uncertainty resulting from experimental error in the measurements taken. Finally, a collection of sample photographs taken during the investigation is presented.

B. Analysis Of Photographic Prints

Each test point produced a series of 20 still photographs. Each print revealed only a fraction of the total number of sites active at that heat flux because the fast shutter speed (1/500 second), the shallow depth of field (.040 inches) and the intermittency of bubble emission from a nucleation site, prevented a single photograph from covering a sufficient period of time to record all of the active sites. Each additional print revealed sites, some of which had not previously been observed, and some of which were simply additional pictures of sites which had been previously shown on earlier photographs. Hence it became necessary to eliminate the duplicate sites in order to obtain an accurate count. A computer program

was devised for this purpose and is described in the next section of this chapter.

A photographic reference grid .407 by .407 inches square was scribed and painted on a transparent acrylic plastic plate which in turn was mounted on the apparatus approximately 0.140 inches below the boiling surface. Though extremely out of focus, this grid cast sufficient shadow to be visible as a size and position reference in the photographic prints. In the final print, this grid was 10 times actual size.**

Depth of field tests* conducted with the lens at a focal length of 8.25 inches, which was the setting used for all photographs taken during the experiment, indicated that grid lines which were located more than .040 inches away from the focus point on a test grid were blurred so much that it was possible to discount the possibility of a bubble .040 inches above the heater surface being visible in the photographic prints. These tests assured that all bubbles depicted in the photographic prints were either still attached to the surface or were immediately above it and hence marking well defined bubbles on the prints was equivalent to identifying and recording the position of active nucleation sites.

---

* See Appendix C.

** Concern arose to the possibility that the grid might not represent its own area on the boiling surface because of paralax. Tests described in Appendix 6 proved this error to be less than one percent.

Each of the photographic prints was analysed in such a manner, taking into consideration the size, shape, definition, position, and shading of the bubbles. The position of those bubbles meeting standards established during preliminary tests were identified and marked as active nucleation sites.

With the active sites identified and marked, each print was then placed on a Benson and Lehner "Oscar" Model 4F Decimal Converter which automatically punched the two dimensional co-ordinates of each identified site onto computer cards. The Converter was programmed to interpret the co-ordinates in thousandths of an inch with reference to the photographic reference grid appearing on each print.

C. Computer Program For Counting Active Sites

Though the decimal converter produced a record of the active nucleation sites identified in the set of twenty photographic prints, it was still necessary to sort out and eliminate those identifications which were duplications. The computer replaced the tedious task of correlating the sites by transferring the co-ordinates of each identified site from one print to the next. The essential features of the program are depicted in the alogarithm shown in Figure (31) of Appendix F.

Each data card containing the x and y co-ordinates of a single identified site was read one by one. The

co-ordinates of the first site were stored automatically. The co-ordinates of the second site were then read from the data and compared with those of the first site. If both the x and y co-ordinates of the second site were the "same" (ie. within a predetermined tolerance limit) as those of the first site, the second site was rejected because it was deemed a duplication of the first. If either the x or y co-ordinates differed by an amount greater than the tolerance limit, the x and y co-ordinates of the site were recorded.

The third set of co-ordinates was then read and compared with those of the previously recorded sites. The process continued until all the cards had been read and then those sites whose co-ordinates had been recorded were totaled up to give the active site count. This figure was multiplied by appropriate scaling factors to produce the active site density per square foot.

The tolerance limit on the difference between the co-ordinates of two identified sites was necessary because the decimal converter could not consistently produce a zero variation between the co-ordinates of the same site appearing on separate photographs. Repeatibility tests indicated that for 100 identified sites recorded and re-recorded by the decimal converter, the variation in the recorded co-ordinates ranged from zero to .011 inches with a mean of .007 inches.

Thus a limit had to be set on the comparison between two sets of co-ordinates as to when they both represented the same site.

In addition, the tolerance became a useful variable parameter by which the computer program could be adjusted to yield active site densities in agreement with visual counts which could be obtained at low heat flux. To establish a realistic tolerance limit, several people were asked to observe Freon 113 boiling at low heat flux and to count the active sites within the reference grid as rapidly as possible. These visual site counts were compared with the counts obtained from twenty photographs taken at the same conditions and processed by the computer counting technique. The tolerance limit was varied and the computer program was found to give results in close agreement with visual counts when the tolerance limit was set at .010 inches.* Counts from the computer were consistantly within 3 percent of the corresponding visual count. As a result of these findings, the .010 inch tolerance limit was adopted and used throughout the entire investigation.

In addition to the initial testing, each time that a new test fluid was introduced, visual counts were

---

* It is interesting to note that the average bubble radius for Freon 113 at saturation conditions is approximately .010 inches.

taken at the low heat flux settings. Agreement between the visual counts and those of the computer was in every instance extremely good (within 3 percent) and served to increase confidence in the combined choice of a .010 inch tolerance limit and a 20 photograph sample for each test point.

D. Analysis Of Experimental Error

In this section, an analysis of the uncertainty in test results introduced through experimental error in the measurements taken is discussed. Each type of data is described with regard to its maximum uncertainty. Where applicable, compound error is computed statistically. The percentage uncertainty in R, a result obtained by combining a number of independent variables V_1, V_2, V_3, ... V_n is given by the formula

$$\frac{W_R}{R} = \left[\left(\frac{\partial R}{\partial V_1}\frac{W_1}{R}\right)^2 + \left(\frac{\partial R}{\partial V_2}\frac{W_2}{R}\right)^2 + \left(\frac{\partial R}{\partial V_3}\frac{W_3}{R}\right)^2 \ldots \left(\frac{\partial R}{\partial V_n}\frac{W_n}{R}\right)^2\right]^{1/2} \quad (17)$$

where W_R is the uncertainty in the result R, and W_1, W_2, W_3, ... W_n is the uncertainty in each of the independent variables.

In addition to the active site densities obtained from the photographs, other measurements were necessary for establishing proper conditions within the test cell and for later use in the evaluation of the Gaertner site activation theory. These measurements and their uncertainty are also discussed. The remainder of the section is divided in four

parts as follows.

1. Uncertainty in the site density data obtained from the photographs.
2. Computation of heat flux leaving the heater surface.
3. Measurement of temperature of the heater surface.
4. Measurement of temperature of the bulk fluid.

1. Uncertainty in the site density data obtained from the photographs.

The techniques used in photographing and counting the active nucleation sites have already been presented along with the tests and observations which provided confidence in their accuracy. Experimental uncertainty results out of possible errors in both the counting technique and the measurement of the heater surface area within the photographic reference grid. A comparison between results obtained from the computer counting technique and visual counts showed the agreement to be consistantly within 3 percent. Possible error in the area of the heater surface described by the reference grid is estimated to be no greater than 5 percent. An analysis of the total uncertainty in active site densities resulting out of a compounding of these two possible errors was computed using Equation (17) to be of the order of ±8 percent.

2. Computation of heat flux leaving the heater surface.

Heat flux from the heater surface was calculated

from the power input determined from the voltmeter and ammeter in the power supplying using the expression

$$\frac{Q}{A} = 3.414 \frac{EI}{A} \tag{18}$$

The values of E and I were corrected for meter error using a calibration curve developed for the power system. In addition, correction had to be made for heat loss from the test surface. Reference (10) describes similar corrections, firstly for heat loss by convection to air underneath the heater surface and secondly for heat loss by conduction from the edges of the heater surface to the test cell.

The experimental apparatus used in the current investigation differed from that described in Reference (10) in that a photographic reference grid scribed in a transparent plastic plate was suspended approximately .015 inches below the underside of the heater surface. The plate created a dead air space in the recess below the heater surface. The grid plate was in turn mounted on a second transparent plastic plate 1/4 inch below it which completely covered the mouth of the recess as shown in Figure (9). This design provided a second dead air space.

Because the upper dead air space was very thin, no attempt was made to measure the temperature of the air contained in it. However the temperature of the air in the lower air space was observed to be less than 6°F above

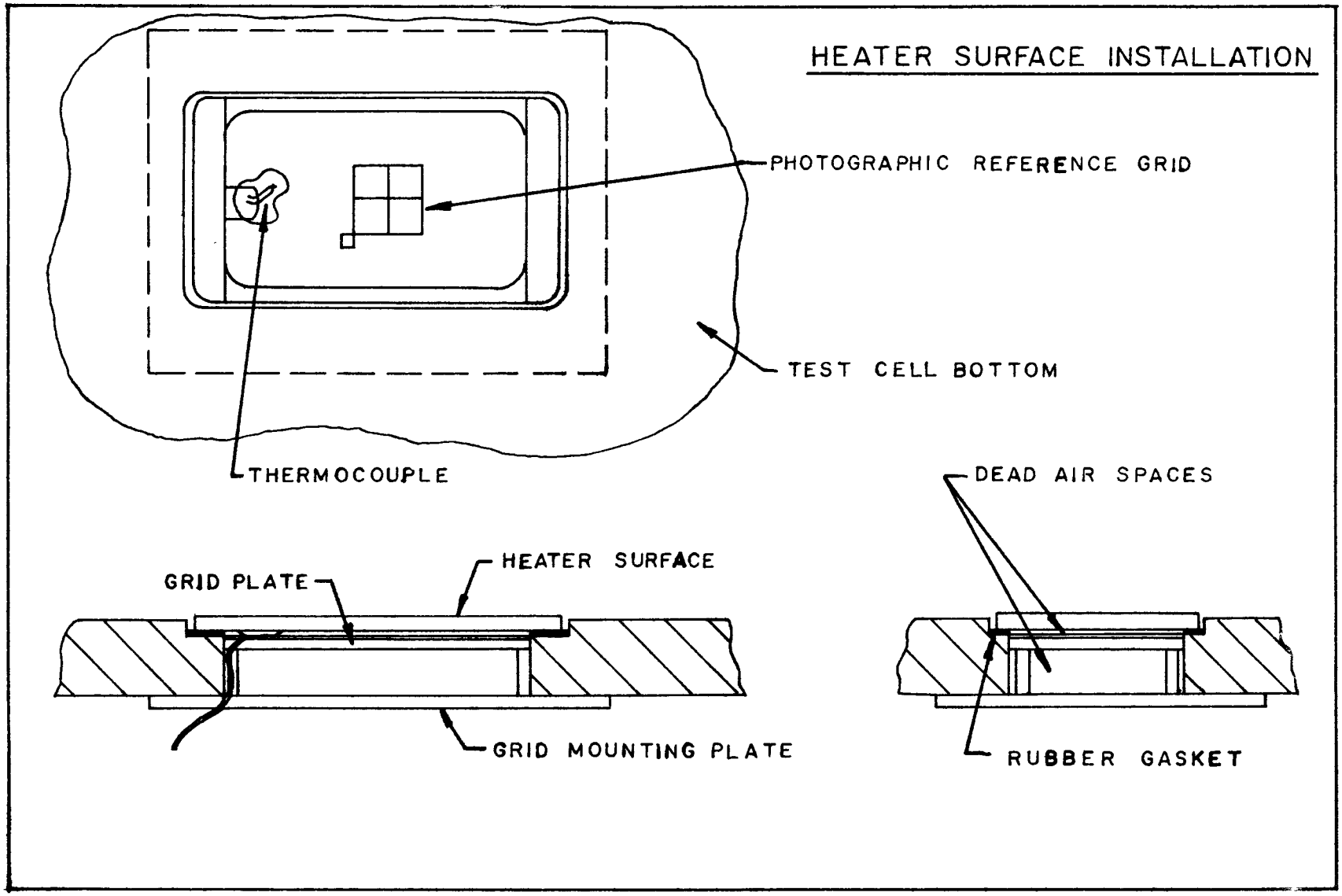

FIGURE 9. HEATER SURFACE INSTALLATION

the saturation temperature of the fluid.* It was deemed a reasonable assumption that the grid, its mounting, and the enclosed air spaces could be considered as a single thermal resistance to the one dimensional flow of heat downward and that no exchange of heat took place between the air spaces and the walls of the recess because of the low temperature difference between them. Thus the total heat loss from the lower surface of the heater was equivalent to the convective heat loss downward from the lowest plastic surface which at highest heat flux was less than 6°F above the saturation temperature of the fluid or approximately 245°F in the most extreme case. Room temperature was recorded at 84°F. Substituting these figures into

$$Nu = 0.14\ (GrPr)^{1/3} \tag{19}$$

which has been advanced by Gupta[13] for convective heat transfer downwards from a horizontal surface produces a total heat flux loss by convection of .19 BTU per hour which represents only .05 percent of the total heat flux. For this reason, heat loss by convection was ignored.

Heat loss by conduction through the edges of the heater surface to the bottom of the test cell was computed

---

* This observation is based upon tests made with trichloroethane during highest heat flux conditions in which T_W was 284°F and T_{SAT} was 239°F.

by analysing the heat conducted through the rubber gasket separating the heater surface from the test cell since the gasket constitutes the major heat flow resistance. The gasket is shown in Figure (9). One dimensional conduction was postulated and the boundary conditions were assumed to be T_W at the heater surface and T_{SAT} at the bottom of the test cell. Both these assumptions are pessimistic in that they constitute conditions somewhat more extreme than would be expected.

The highest temperature difference $T_W - T_{SAT}$ observed during the investigation was 46°F. The thermal conductivity* of the rubber gasket was .077 BTU per hour per foot per degree Farenheit. The thickness of the gasket was 1/32 inch and the total contact area was .01096 square feet. These figures produced a maximum heat loss of 14.9 BTU per hour which was 4.0 percent of the total heat flux at the test conditions. This loss was considered sufficient to warrant a correction of the heat flux calculation.

The resultant heat flux equation was thus

$$\frac{Q}{A} = 3.414 \frac{EI}{A} - \frac{Q_{LOSS}}{A} \qquad (20)$$

An analysis of the uncertainty in Q/A as computed by Equation (20) performed using Equation (17) indicated that the

---

* From manufacturers specifications.

Maximum uncertainty in Q/A is of the order of ±5.00 percent assuming a ±50 percent uncertainty in the heat loss correction and an uncertainty in E and I equal to the highest observed meter error of 4.0 percent.

3. Measurement of temperature of the heater surface.

As described in Chapter IV the temperature of the heater surface was measured by a thermocouple epoxyed to the lower surface of the glass. Uncertainty in the temperature measurement arises out of the possibility of a temperature drop through the thickness of the glass resulting from the transfer of heat from the lower surface to the air-space below it.

As has already been explained, heat loss by convection was small but at maximum heat flux levels, analysis of the heat transfer to the air space indicated that the temperature drop across the thickness of the glass could be as high as 0.35°F. Such a deviation is insignificant when T_W is used in the Gaertner equation because it is converted to the Kelvin temperature scale.

4. Measurement of the temperature of the bulk fluid.

Bulk fluid temperature was measured by three probe type thermocouples described in Chapter IV. At saturation conditions the temperature difference between the three

thermocouples was a maximum of 0.20°F and fluctuation in the reading of any single thermocouple was undetectable. During all test runs, bulk temperature of the fluid was recorded as being within 0.20°F of the predicted saturation temperature of the fluid.

E. Sample Photographs

The photographs presented in Figures (10 - 14) are presented with no discussion other than the titles which appear below them. These photographs are considered representative of the prints used in determining the active site density results presented in Chapter VIII.

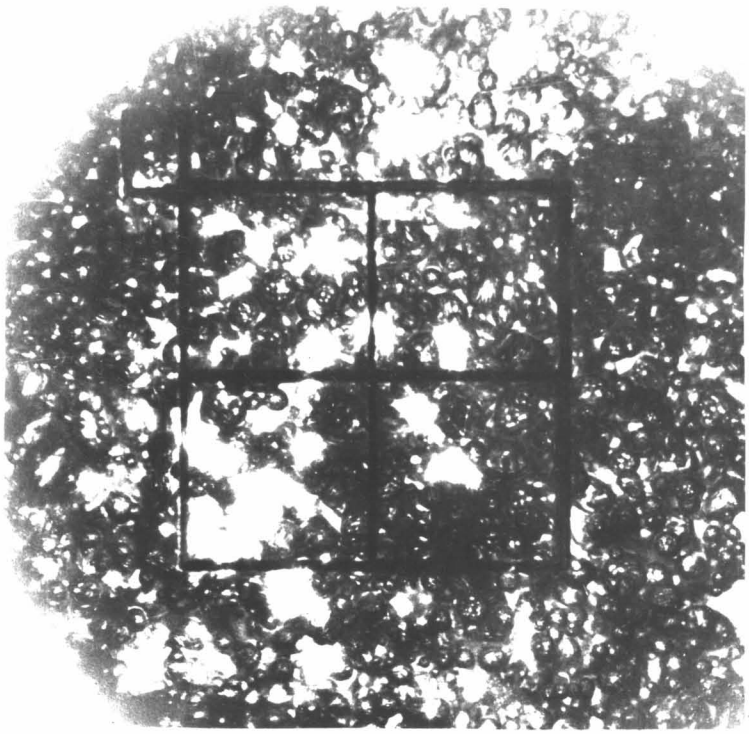

FIGURE 10: SAMPLE PHOTOGRAPH OF FREON113
BOILING AT ATMOSPHERIC PRESSURE
HEAT FLUX: 5,124 BTU/HR.FT^2
ENLARGEMENT FACTOR: 5X(ACTUAL SIZE)

FIGURE 11: SAMPLE PHOTOGRAPH OF CARBON-
TETRACHLORIDE BOILING AT
ATMOSPHERIC PRESSURE
HEAT FLUX: 8,230 BTU/HR.FT^2
ENLARGEMENT FACTOR: 5X(ACTUAL SIZE)

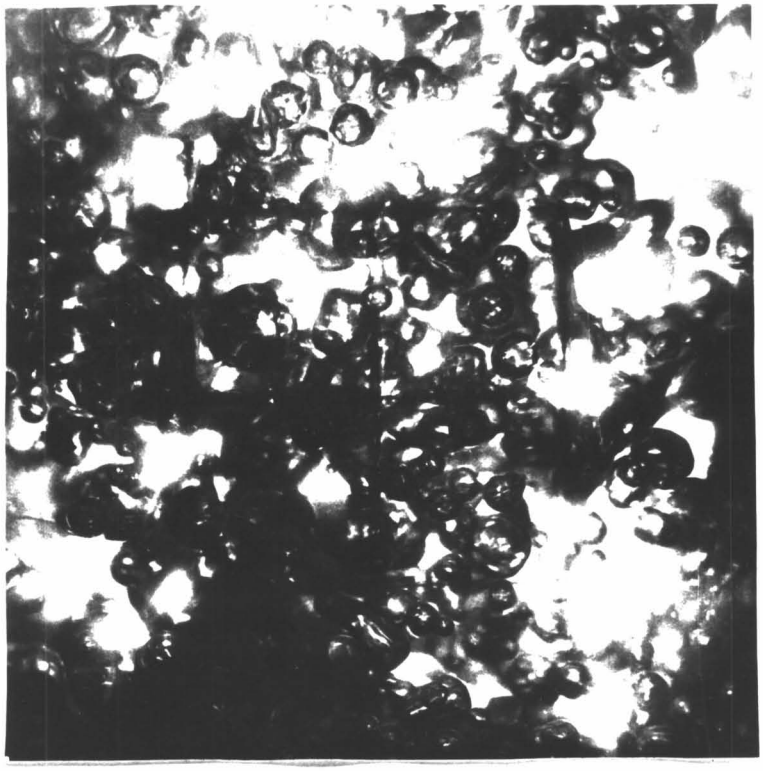

FIGURE 12: SAMPLE PHOTOGRAPH OF CHLOROFORM
BOILING AT ATMOSPHERIC PRESSURE
HEAT FLUX: 11,280 BTU/HR.FT^2
ENLARGEMENT FACTOR: 5X(ACTUAL SIZE)

FIGURE 13: SAMPLE PHOTOGRAPH OF DICHLOROETHANE BOILING AT ATMOSPHERIC PRESSURE

HEAT FLUX: 15,390 BTU/HR.FT^2

ENLARGEMENT FACTOR: 5X(ACTUAL SIZE)

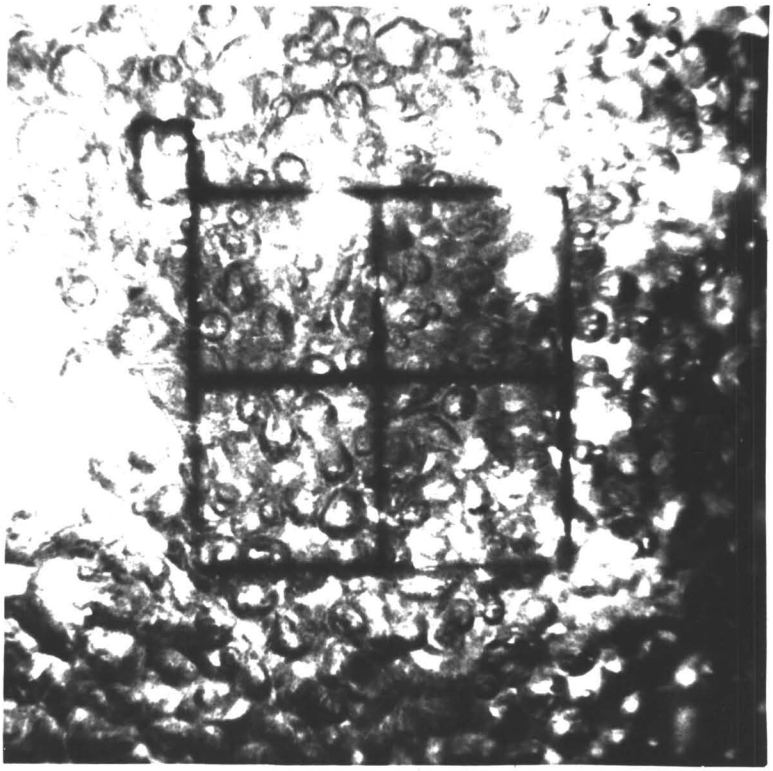

FIGURE 14: SAMPLE PHOTOGRAPH OF TRICHLOROETHANE
BOILING AT ATMOSPHERIC PRESSURE
HEAT FLUX: 20,150 BTU/HR.FT^2
ENLARGEMENT FACTOR: 5X(ACTUAL SIZE)

CHAPTER VIII

EXPERIMENTAL RESULTS

The results of the current investigation are presented in this chapter without comment. Discussion and interpretation of the results is given in Chapter IX and the manner in which the data was reduced to meaningful results has already been presented. The data for each test series is presented on a single page combining three graphs.

The first graph is a plot of heat flux versus superheat, the classical manner in which saturated boiling heat transfer results are plotted. The second graph plots active site density against superheat and the last graph is a plot of active site density versus heat flux.

The three graphs for each fluid have been placed together for quick reference. No attempt was made at this point to superimpose the results of the various test series because the resulting graphs would be extremely cluttered. Correlation of the data is discussed in the next chapter.

The results of the reproducibility test for Freon 113 conducted in Test Series 6 are shown with the original data for Freon 113 in Figure (15). Reproducibility of the active site density was within 1.84 percent of the original data.

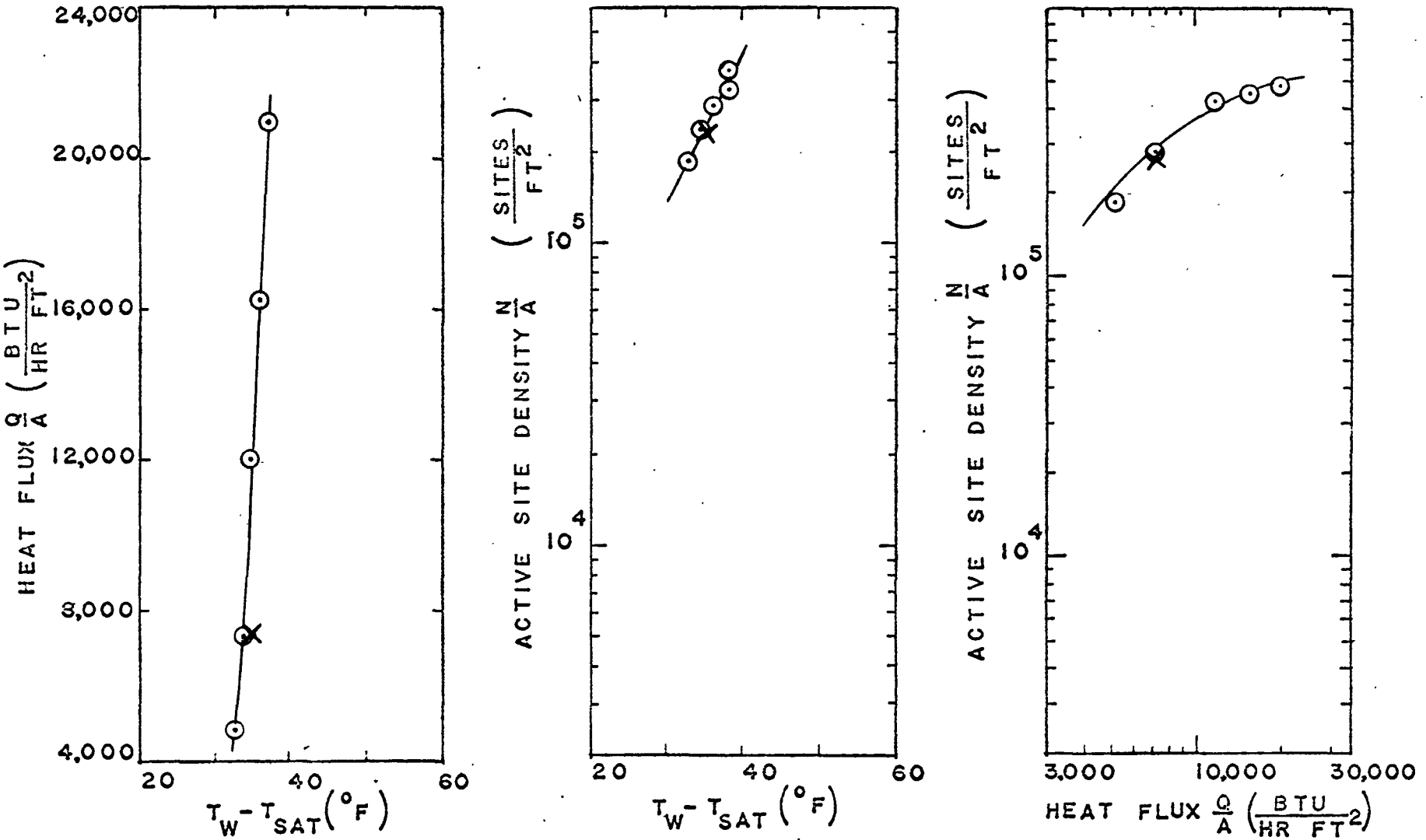

X DATA FROM REPRODUCIBILITY TEST

T_{SAT} = 117.8 °F

FIGURE 15. DATA FOR FREON113

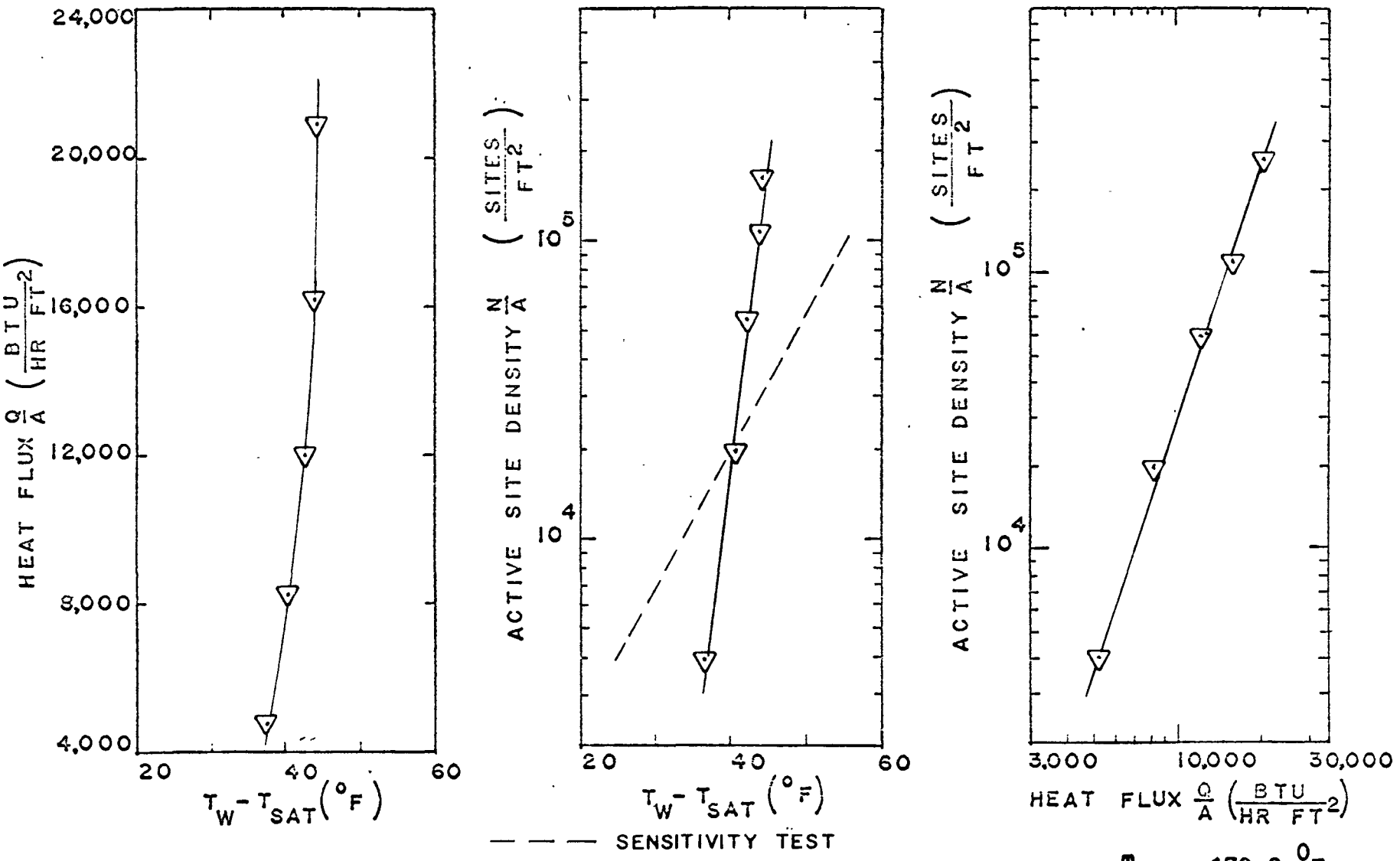

FIGURE 16. DATA FOR CARBON-TETRACHLORIDE

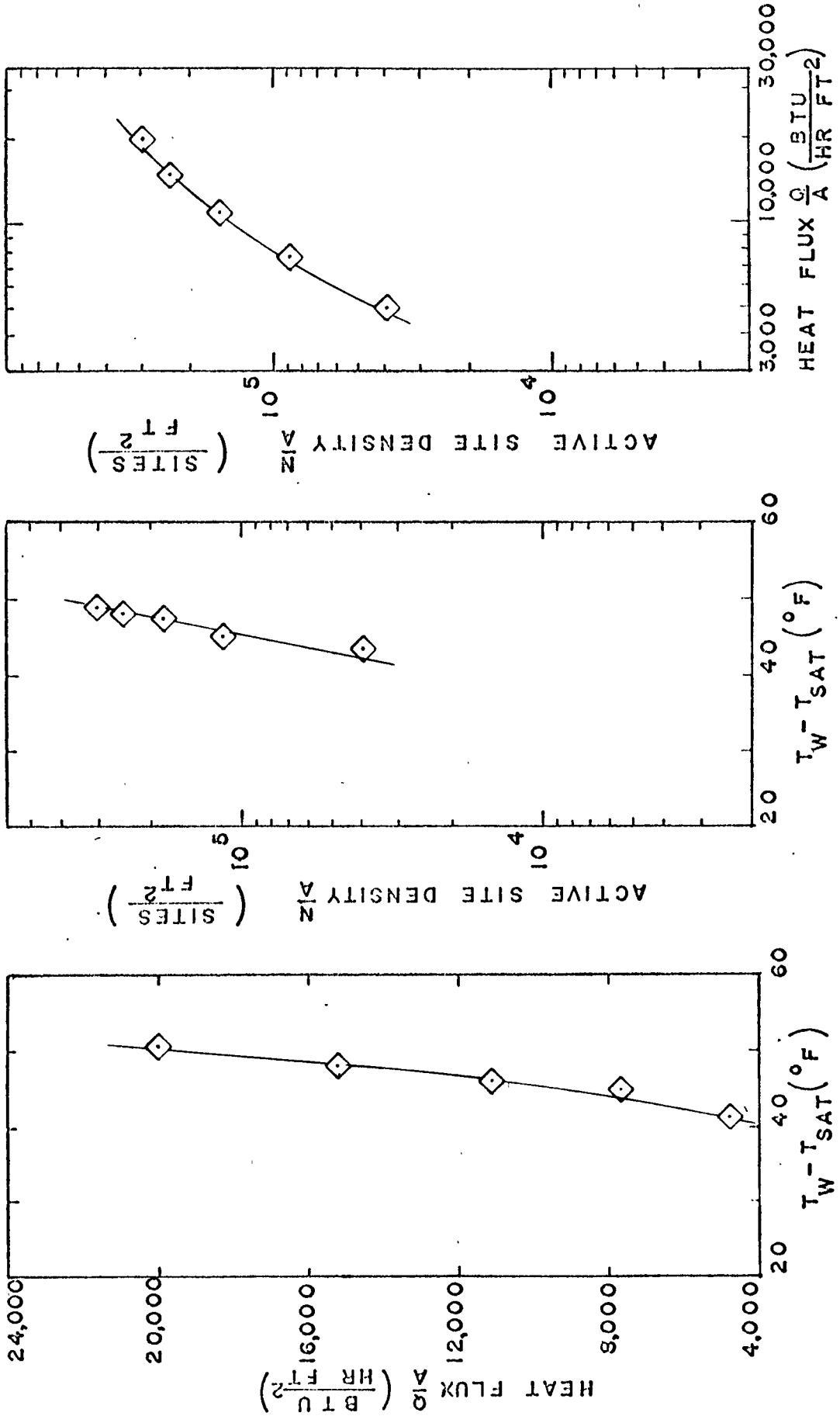

FIGURE 17. DATA FOR CHLOROFORM

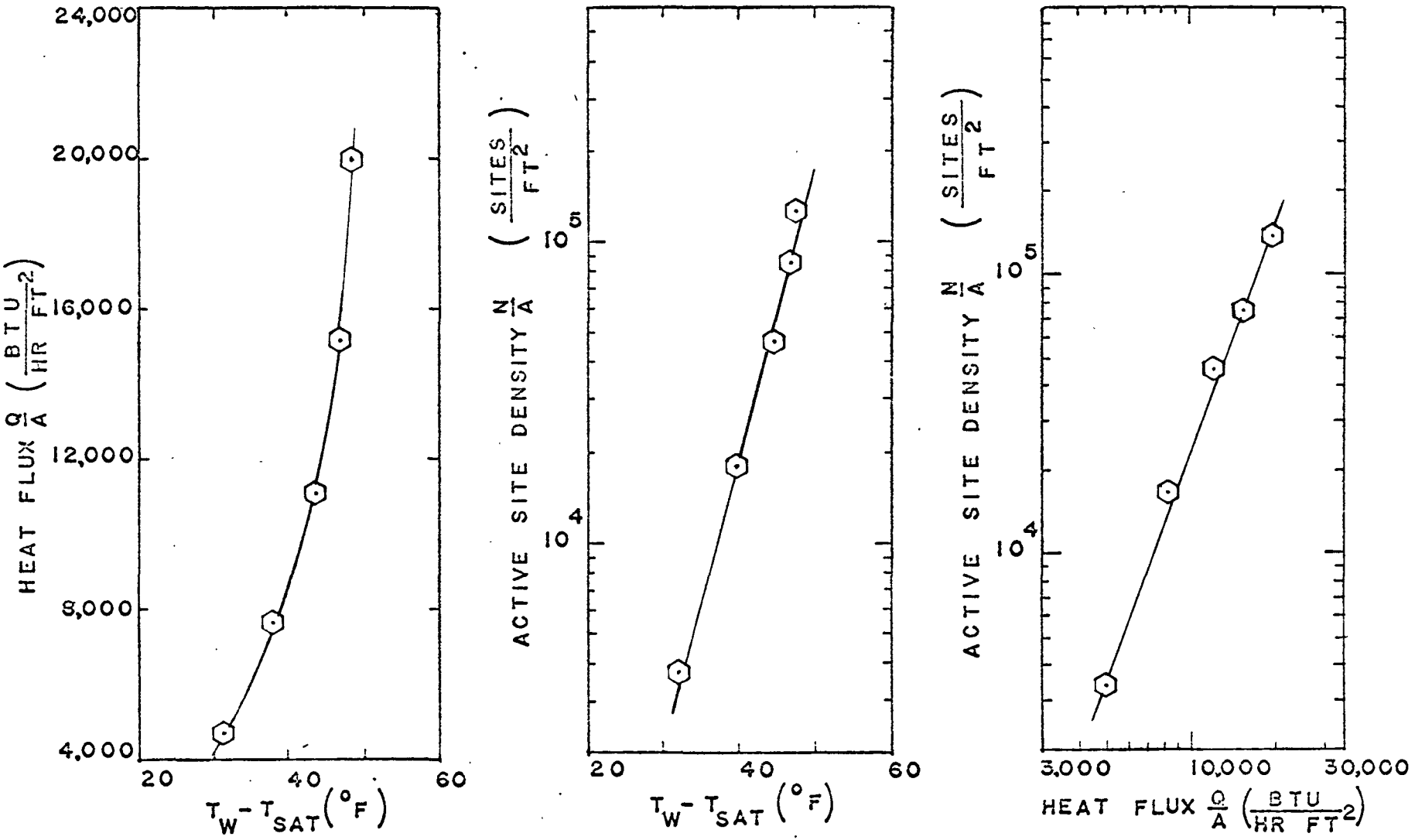

$T_{SAT} = 180.1\ ^{0}F$

FIGURE 18. DATA FOR DICHLOROETHANE

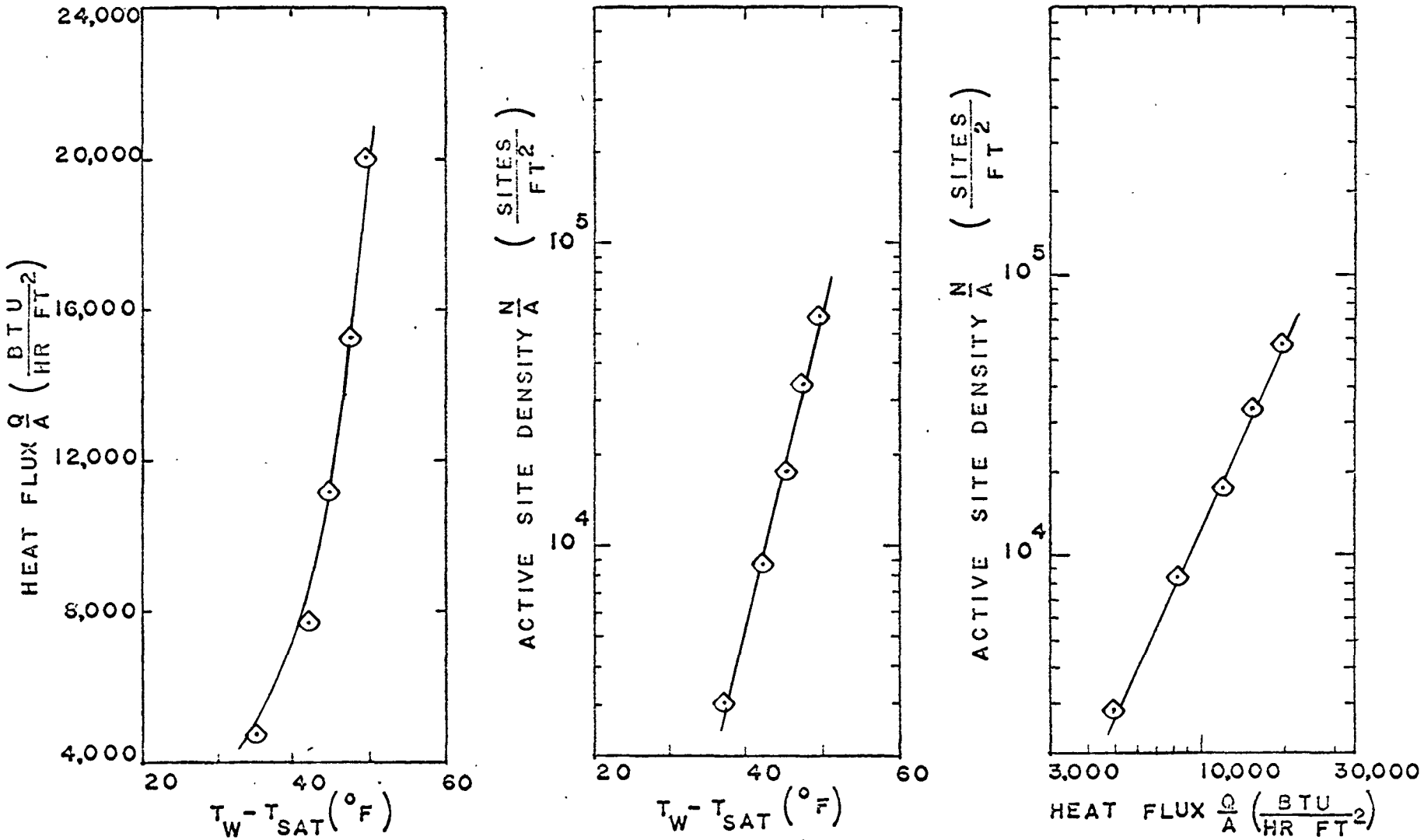

FIGURE 19. DATA FOR TRICHLOROETHANE

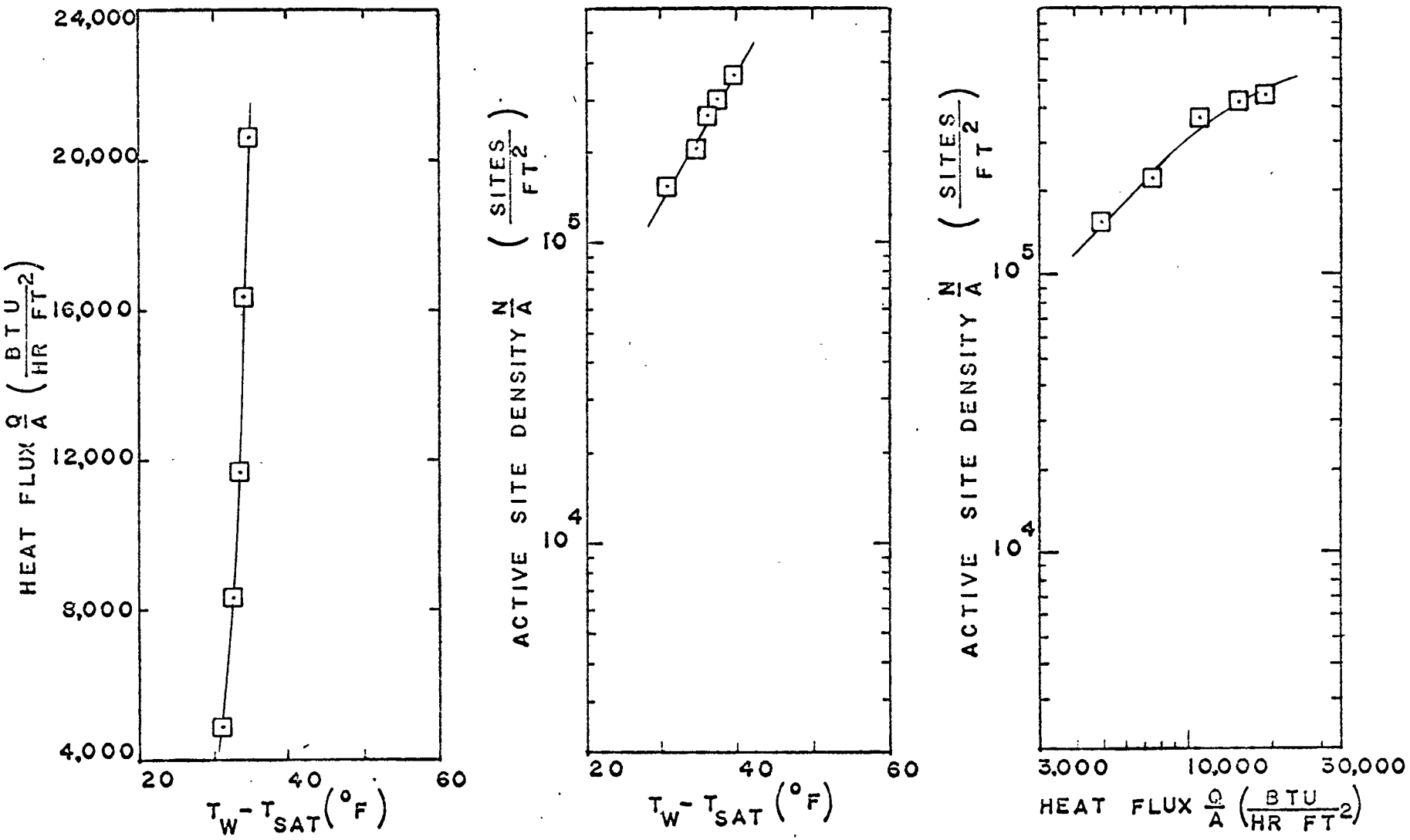

$T_{SAT} = 142.0\ ^0F$

FIGURE 20. DATA FOR FREON113 BOILED WITH HELIUM OVER-PRESSURE

CHAPTER IX

DISCUSSION

The purpose of the current investigation has been stated as obtaining site density data for five different fluids boiling on a single transparent heater surface with a view to evaluating Gaertner's site activation theory. This theory has been extensively treated in Chapter III and the final expression need only be presented here.

$$\frac{N}{A} = N_o \exp\left\{ -\left(\frac{16\pi\sigma^3 M^2 N^*}{3\rho_L{}^2 R^3 [\ln(\frac{P_\infty}{P_v})]^2} \right) \Phi \left(\frac{1}{T_w{}^3}\right) \right\} \qquad (1)$$

As mentioned in the introduction, this equation contains two arbitrary constants N_o and Φ which must be evaluated empirically for each fluid-surface combination. Gaertner used the only existing set of data drawn from Reference (7) to test the correlation. Although he was able to confirm the effect of wall temperature on the active site density, Gaertner could not investigate the influence of fluid properties upon active site density without additional data. Using the Gaertner equation, Judd[10] correlated his data for Freon 113 boiling on a transparent glass heater surface and also that of Kirby and Westwater[8] for carbon-tetrachloride boiling on a similar surface.

An interesting observation resulted from Judd's

work. It was demonstrated that the product $\left(\frac{16\pi\sigma^3 M^2 N^*}{3\rho_L{}^2 R^3 [\ln(\frac{P_\infty}{P_v})]^2}\right)\Phi$ was almost constant for the three correlated sets of data. This observation implies that the Gaertner equation can be simplified to

$$\frac{N}{A} = N_o \exp\left\{-\frac{K}{T_W{}^3}\right\} \qquad (21)$$

where K is a universal constant independent of the fluid properties.

The data obtained in the current experiment was correlated using the Gaertner equation to tests Judd's hypothesis. The logarithms of the active site densities were plotted against the inverse surface temperature cubed. The resulting correlation is shown in Figure (21). The straight line correlation through each data set indicates that the active site density varies with the exponential of the inverse temperature cubed as predicted by the Gaertner theory. Also included on the graph are the results of Judd for Freon 113, Kirby and Westwater for carbon tetrachloride, and Gaertner for an aqueous nickel salt solution, all of which are presented in Reference (10).

Figure (21) substantiates the hypothesis that $\left(\frac{16\pi\sigma^3 M^2 N^*}{3\rho_L{}^2 R^3 [\ln(\frac{P_\infty}{P_v})]^2}\right)\Phi$ is constant, at least for the same

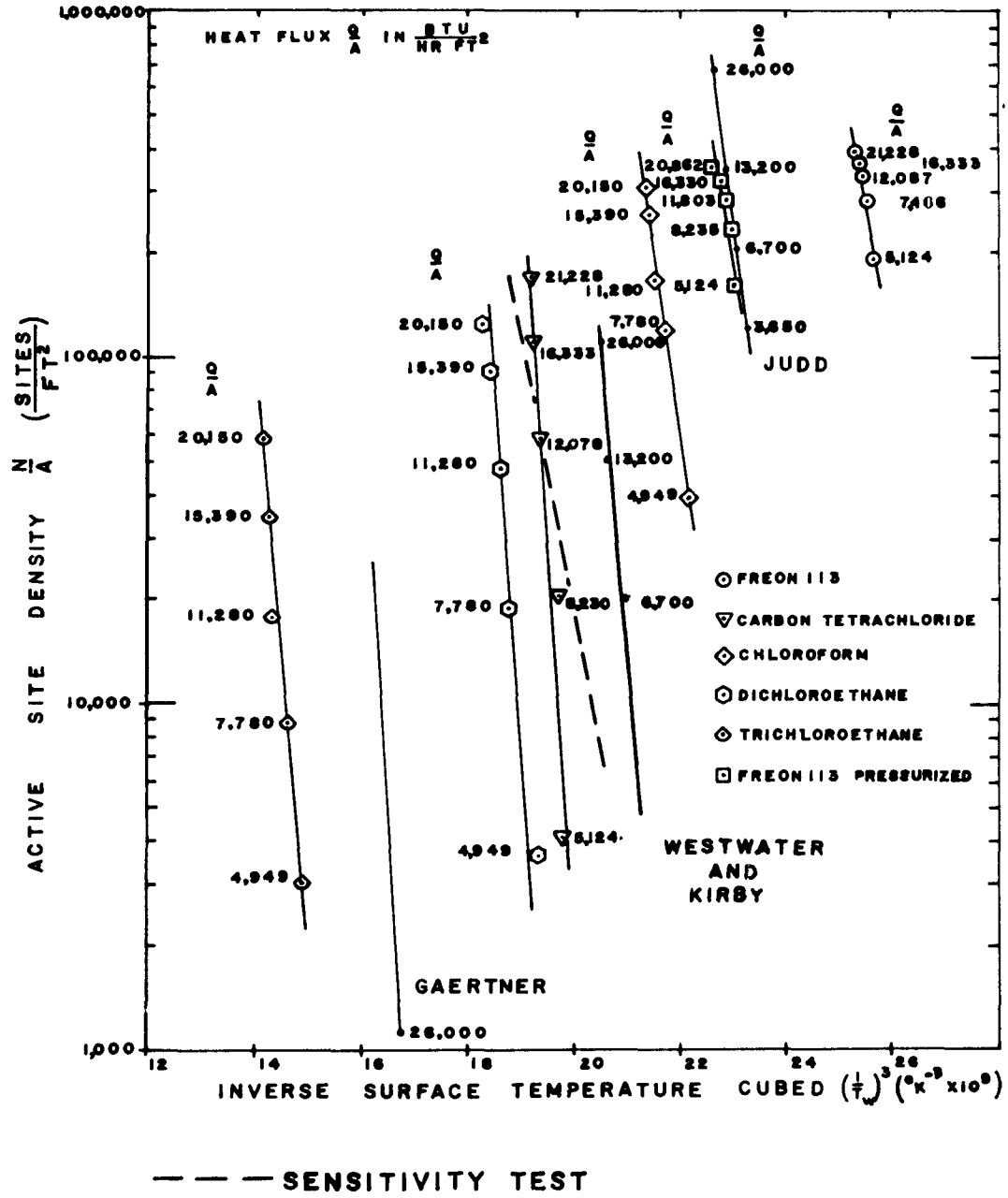

FIGURE 21. EVALUATION OF GAERTNER SITE ACTIVATION THEORY

surface. The straight lines drawn through each set of plotted data were made without reference to each other to avoid prejudging their parallelism and yet they do appear nearly parallel indicating that indeed the product $\left(\frac{16\pi\sigma^3 M^2 N^*}{3\rho_L^2 R^3 [\ln(\frac{P_\infty}{P_v})]^2}\right)\Phi$ approaches a constant.

To test the significance of this observation, a statistical test was performed on the data using a digital computer. A first order least squares analysis was performed on each set of data. This analysis resulted in a slope for the best fitted straight line through each data set and the minimum square deviation in each set. Next, the slope of the best single straight line fitted through all the sets of data, hereafter referred to as the pooled slope line, was computed and again the minimum square deviation in all the sets was obtained.

In both the case of the individually fitted lines and the pooled slope line, the standard deviation and variance for the five sets of data was computed. Finally, a variance ratio test (or F test) was performed on the variance occurring between the individually fitted slopes versus the mean difference between the common pooled slope and each of the individually fitted slopes using the formula outlined in

Moroney[14].

$$F = \frac{\text{variance of the estimate}}{\text{variance of the error of the estimate}}$$

or in this case

$$F = \frac{\text{variance between individual slopes}}{(\text{pooled slope} - \text{individual slopes})_{\text{mean}}} \qquad (22)$$

The variance ratio test was first performed on the five sets of data corresponding to the five fluids boiled at atmospheric pressure in the experiment. Equation (22) produced a variance ratio F = 1.2975 which for the degrees of freedom* of the system indicated that there was no significant difference between the slope of the individually fitted lines and the pooled slope line at the 95 percent probability level since for the same degrees of freedom, F could be as great as 5.87 by random chance alone. Thus it may be concluded that the lines are representative of an infinite family of parallel lines and that the slopes deviate from the pooled slope because of scatter in the data points**. This implies that the product

---

** Concern arose as to the sensitivity of the Gaertner correlation to small changes in T_W. This sensitivity is discussed in Appendix I.

* Degrees of freedom for numerator = 15
Degrees of freedom for denominator = 4

$\left(\frac{16\pi\sigma^3 M^2 N^*}{3\rho_L^2 R^3 [\ln(\frac{P_\infty}{P_v})]^2} \right) \Phi$ is constant irrespective of the fluid properties.

The addition of the data for Freon 113 at 8 pounds per square inch gauge pressure and the data for the same conditions reported in Reference (10) did not change the outcome of the variance ratio test appreciably. Thus $d[\ln \frac{N}{A}]/d[\frac{1}{T_W^3}]$, the slope of the pooled slope line through the seven sets of data, may be used as the constant K of the proposed simplified Equation (21). The value of K was found to be $3.305 \times 10^9 °K^3$ which is in good agreement with the value of $3.0 \times 10^9 °K^3$ suggested by Judd[10]. The constant K is independent of the properties of the fluid being boiled and its use in Equation (21) predicts the active site density within ±8 percent for the boiling of all fluids on an oxide coated glass surface.

The remaining question is whether K is dependent of the surface properties or is in fact a truly universal constant for all fluid-surface combinations. Comparison of the correlations for Gaertner's results and for Kirby and Westwater's results which are included in Figure (21) suggests that the slopes of these two lines differ little from

the rest. However, Kirby and Westwater's results for carbon tetrachloride were obtained by boiling on a surface very similar to that used in the current investigation and Gaertner's results for a nickel salt solution boiling on copper could not be statisitically analysed since the numerical values upon which the correlations were based are not readily available. Additional data for other surfaces would be needed before any definite conclusions could be drawn on the effect of surface properties on the active site density.

CHAPTER X

CONCLUSIONS

1. Extensive active site density results were obtained for five fluids during this investigation. Three of the fluids; chloroform, dichloroethane, and trichloroethane, had not been previously investigated. While there have been numerous early investigations which reported site density data at very low heat flux, the current data in addition to that of Gaertner[1], Judd[10], and Kirby and Westwater[8], is the only extensive data at sufficiently high heat flux to be useful in the evaluation of heat transfer models.
2. Data obtained for Freon 113 is in good agreement with the results reported by Judd[10] for the same set of conditions.
3. The Gaertner site activation theory correlates the data obtained in this investigation well. While the Gaertner equation cannot predict the active site density without previous empirical evaluation of the arbitrary constants N_o and ϕ for each fluid-surface combination, the analysis performed in this investigation indicates that the product $\left(\frac{16\pi\sigma^3 M^2 N^*}{3\rho_L^2 R^3 [\ln(\frac{P_\infty}{P_v})]^2}\right)\phi$ is independent of fluid properties for a particular surface.
4. Although the analysis was inconclusive, it appears possible that the product $\left(\frac{16\pi\sigma^3 M^2 N^*}{3\rho_L^2 R^3 [\ln(\frac{P_\infty}{P_v})]^2}\right)\phi$ might be a truly universal constant, independent of both fluid and surface properties.

A P P E N D I X A

THE BOILING REGIMES

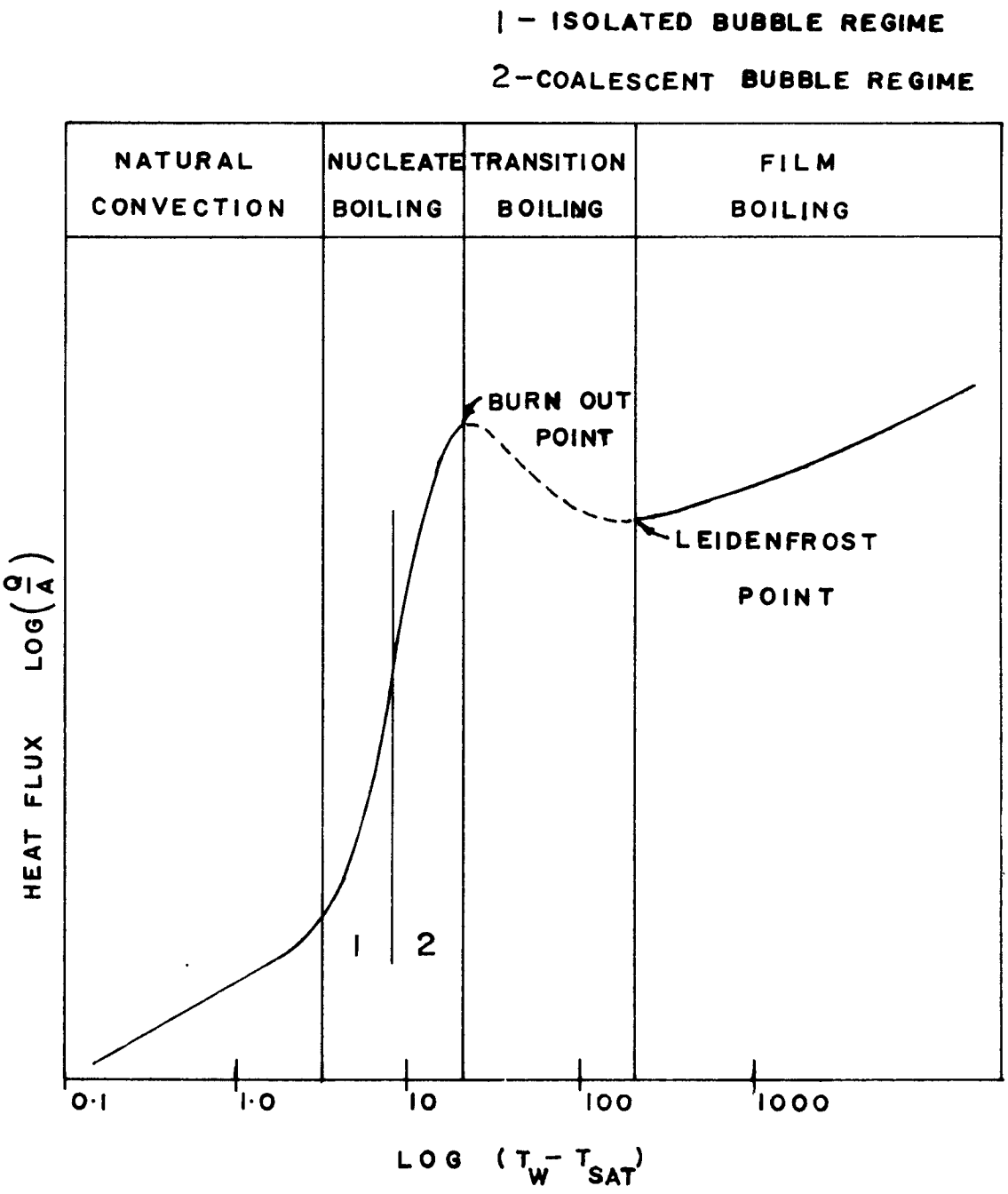

FIGURE 22:

BOILING HEAT TRANSFER REGIMES

A P P E N D I X B

METER CALIBRATION ON POWER SUPPLY

Meter Calibration On Power Supply

Uncertainty in the calculation of power input to the heater surface arose out of possible inaccuracy of the volt meter and ammeter in the output circuit of the D.C. power supply. A series of calibration tests of the meters was conducted using a VTVM voltmeter and fixed resistances whose values were known to be within 0.5 percent. The calibration curve shown in Figure (8) was developed by applying increasing increments of current from the power system across the known resistances and measuring the voltage readings with both the VTVM and the voltmeter of the power system. The calibration curve could thus be used with current readings from the ammeter on the power system.

To compensate for error in the ammeter, the resistance of the heated surface was plotted on the calibration chart. All heater surfaces were within 0.1 ohms of the 32 ohm resistance line.

A P P E N D I X C

PHOTOGRAPHIC DEPTH OF FIELD TEST

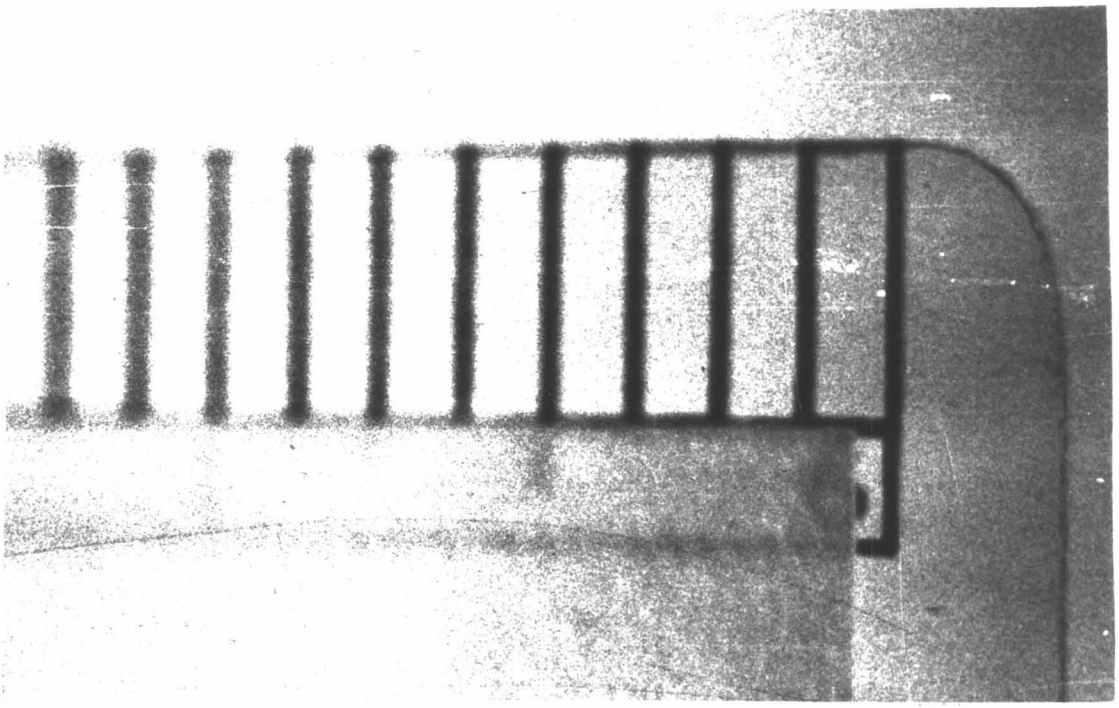

FIGURE 23:

DEPTH OF FIELD TEST OF CLOSE-UP LENS

FOCAL LENGTH SETTING FOR THIS TEST WAS 8.25 INCHES. LENS WAS FOCUSED ON THE EXTREME RIGHT HAND VERTICAL GRID LINE. EACH SUCCEEDING LINE TO THE LEFT IS .005 INCHES BEHIND THE ONE TO ITS RIGHT. AS CAN BE SEEN, LINES MORE THAN .040 INCHES BEHIND THE FOCAL POINT ARE EXTREMELY BLURRED.

A P P E N D I X D

DATA TABULATION

TABLE 2

TEST DATA

TEST SERIES	TEST POINT	FLUID	$\frac{Q}{A}$ BTU/HR.FT.^{2}	P_T PSIA	T_{SAT} ^0F	T_W ^0F	T_B ^0F	BUBBLE COUNT PER FT.^{2}
1	1	FREON113	5124	14.80	117.8	150.3	116.9	196992
1	2	"	7466	14.80	117.8	151.8	117.3	281664
1	3	"	12078	14.80	117.8	152.5	117.3	333504
1	4	"	16333	14.80	117.8	152.9	117.3	355104
1	5	"	21228	14.80	117.8	153.4	117.3	393120
2	1	CCl_4	5124	14.49	170.2	205.6	169.5	4026
2	2	"	8230	14.49	170.2	210.2	169.7	20416
2	3	"	12078	14.49	170.2	212.3	169.7	56741
2	4	"	16333	14.49	170.2	213.6	169.7	110628
2	5	"	21228	14.49	170.2	213.9	169.7	169062
3	1	CHLOROFORM	4949	14.72	141.0	181.9	140.2	39744
3	2	"	7780	14.72	141.0	186.2	140.5	120096
3	3	"	11280	14.72	141.0	187.6	140.5	186624
3	4	"	15390	14.72	141.0	188.7	140.5	253152
3	5	"	20150	14.72	141.0	188.9	140.5	304128
4	1	FREON113	7466	14.50	116.9	151.4	116.3	276480
5	1	DICHLORO-ETHANE	4949	14.62	180.1	210.7	178.9	3649
5	2	"	7780	14.62	180.1	218.7	179.5	18640
5	3	"	11280	14.62	180.1	224.2	179.6	46285
5	4	"	15390	14.62	180.1	226.6	179.6	89992
5	5	"	20150	14.62	180.1	227.0	179.6	122148
6	1	TRICHLORO-ETHANE	4949	14.52	237.8	272.7	236.2	3028
6	2	"	7780	14.52	237.8	278.7	236.7	8688
6	3	"	11280	14.52	237.8	282.0	236.9	17890
6	4	"	15390	14.52	237.8	284.4	237.0	34100
6	5	"	20150	14.52	237.8	285.4	237.0	58048
7	1	FREON113	5124	22.72	142.0	173.6	141.1	160124
7	2	"	8235	22.72	142.0	174.8	141.5	232310
7	3	"	11803	22.72	142.0	175.6	141.6	281298
7	4	"	16330	22.72	142.0	176.1	141.6	322673
7	5	"	20862	22.72	142.0	176.5	141.6	351169

A P P E N D I X E

TYPICAL BUBBLE PHOTOGRAPHS

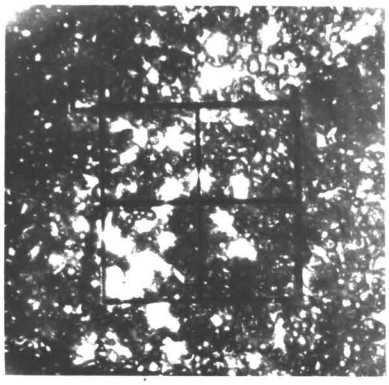

5,124 BTU/HR.FT.^{2}

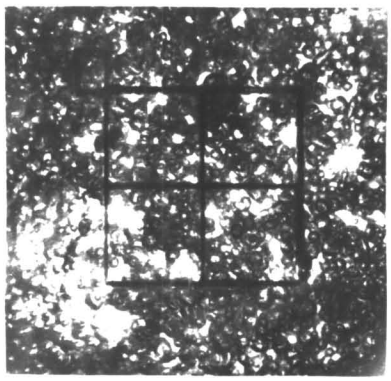

7,466 BTU/HR.FT.^{2}

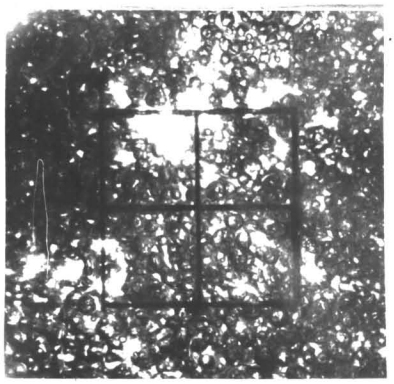

12,087 BTU/HR.FT.^{2}

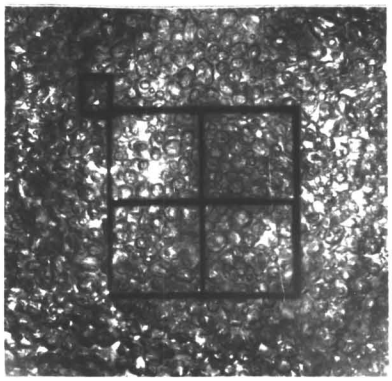

16,333 BTU/HR.FT.^{2}

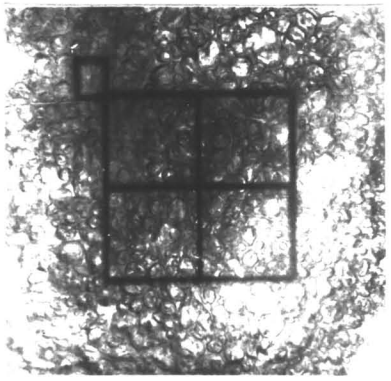

21,228 BTU/HR.FT.^{2}

FIGURE 24:

TYPICAL BUBBLE PHOTOGRAPHS

FLUID: FREON113

PRESSURE: ATMOSPHERIC

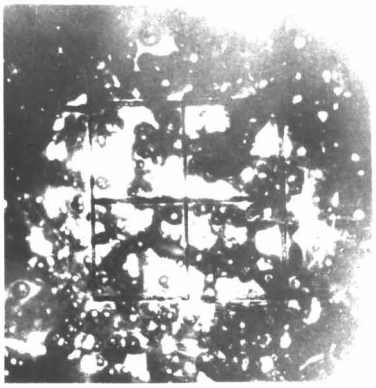

5,124 BTU/HR.FT.^{2}

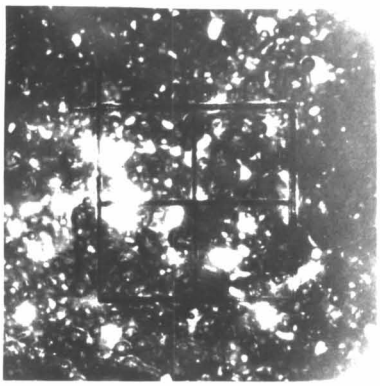

8,230 BTU/HR.FT.^{2}

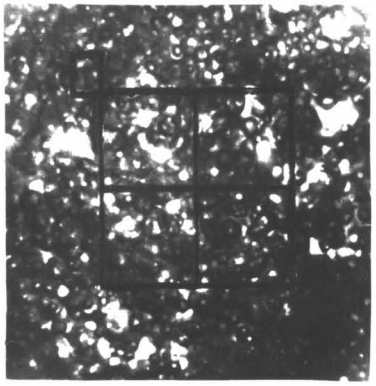

12,078 BTU/HR.FT.^{2}

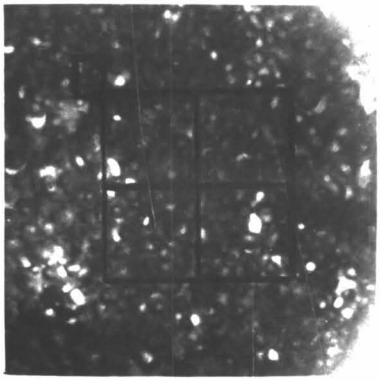

16,333 BTU/HR.FT.^{2}

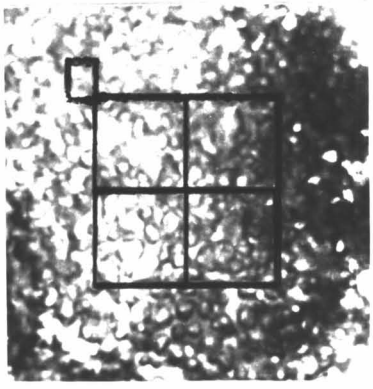

21,228 BTU/HR.FT.^{2}

FIGURE 25:

TYPICAL BUBBLE PHOTOGRAPHS

FLUID: CARBONTETRACHLORIDE

PRESSURE: ATMOSPHERIC

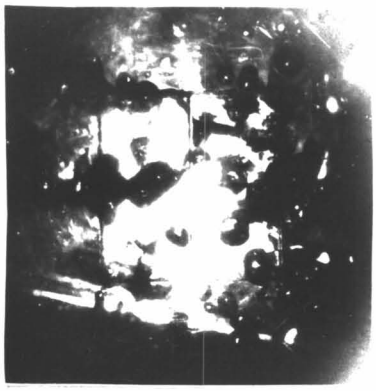

4,949 BTU/HR.FT.^{2}

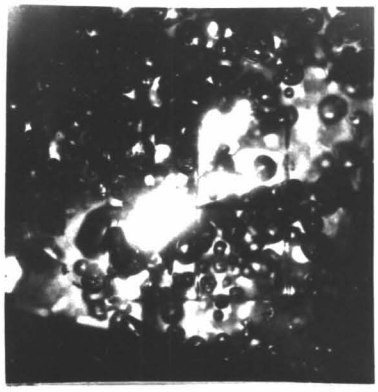

7,780 BTU/HR.FT.^{2}

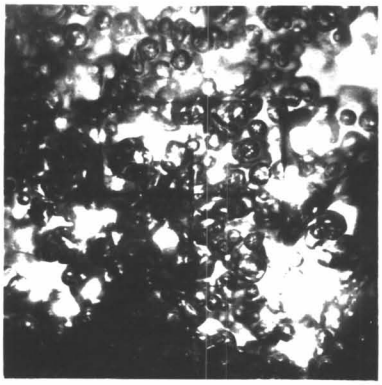

11,280 BTU/HR.FT.^{2}

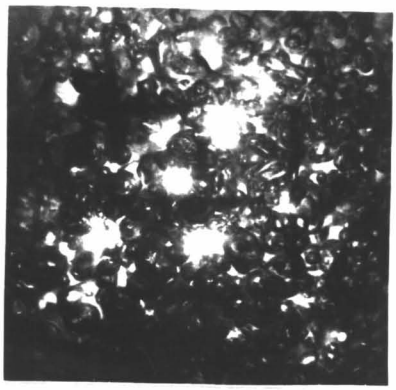

15,390 BTU/HR.FT.^{2}

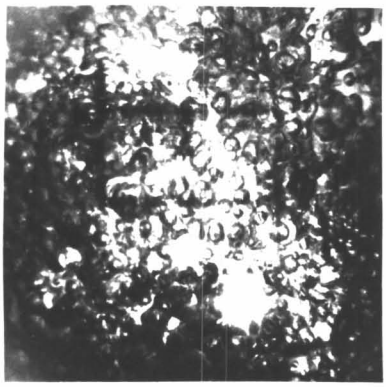

20.150 BTU/HR.FT.^{2}

FIGURE 26:

TYPICAL BUBBLE PHOTOGRAPHS

FLUID: CHLOROFORM

PRESSURE: ATMOSPHERIC

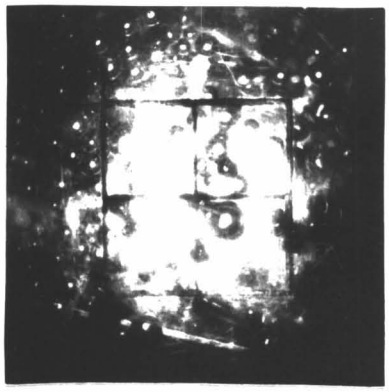

4,949 BTU/HR.FT.^{2}

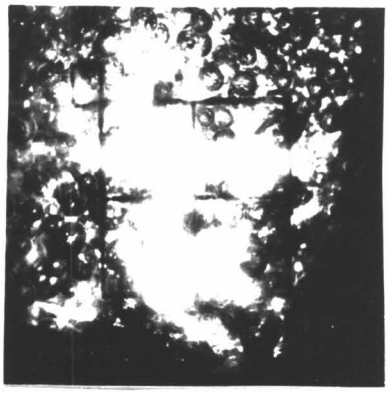

7,780 BTU/HR.FT.^{2}

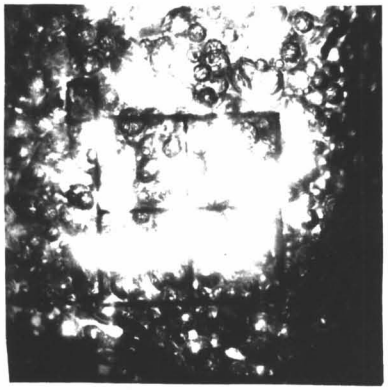

11,280 BTU/HR.FT.^{2}

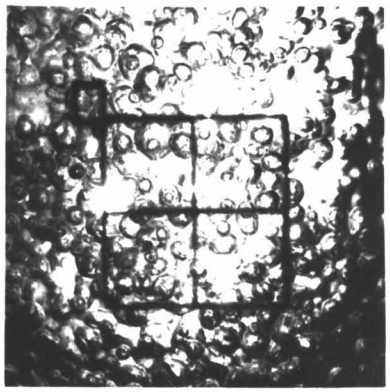

15,390 BTU/HR.FT.^{2}

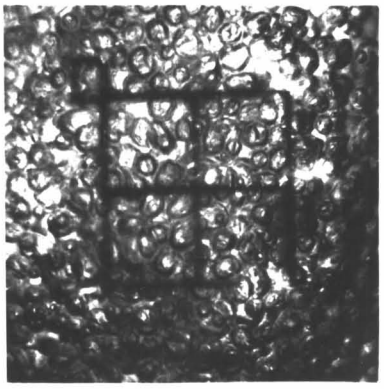

20,150 BTU/HR.FT.^{2}

FIGURE 27:

TYPICAL BUBBLE PHOTOGRAPHS

FLUID: DICHLOROETHANE

PRESSURE: ATMOSPHERIC

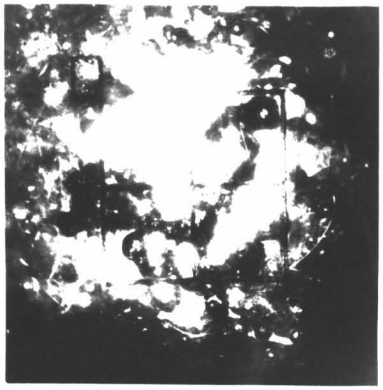

4,949 BTU/HR.FT.^{2}

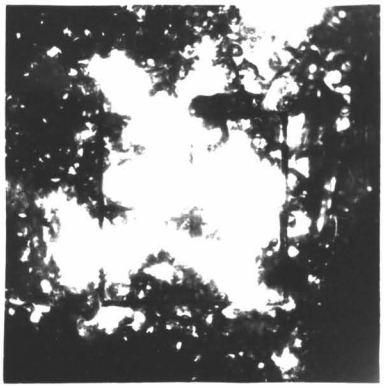

7,780 BTU/HR.FT.^{2}

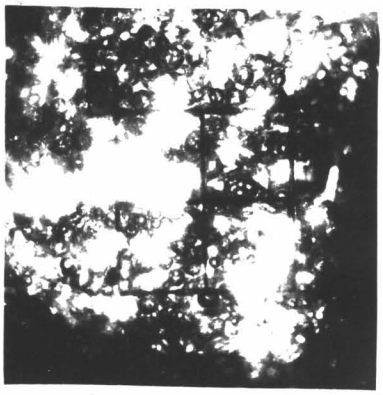

11,280 BTU/HR.FT.^{2}

15,390 BTU/HR.FT.^{2}

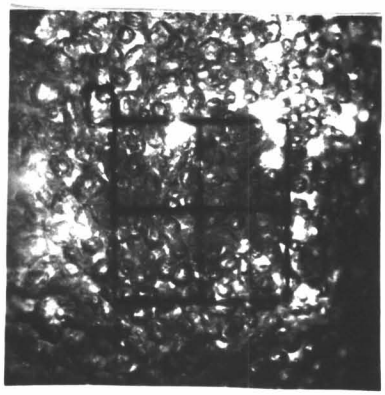

20,150 BTU/HR.FT.^{2}

FIGURE 28:

TYPICAL BUBBLE PHOTOGRAPHS

FLUID: TRICHLOROETHANE

PRESSURE: ATMOSPHERIC

5,124 BTU/HR.FT.^{2}

8,235 BTU/HR.FT.^{2}

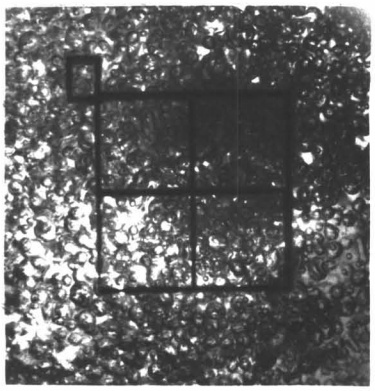

11,803 BTU/HR.FT.^{2}

16,330 BTU/HR.FT.^{2}

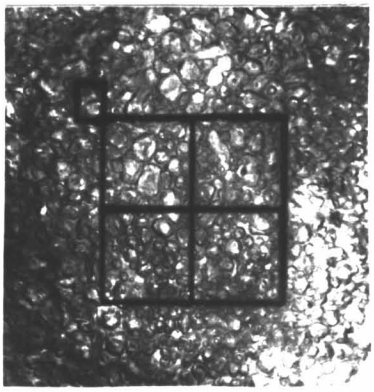

20,862 BTU/HR.FT.^{2}

FIGURE 29:

TYPICAL BUBBLE PHOTOGRAPHS

FLUID: FREON113

PRESSURE: 8 POUNDS PER INCH^2
HELIUM OVERPRESSURE

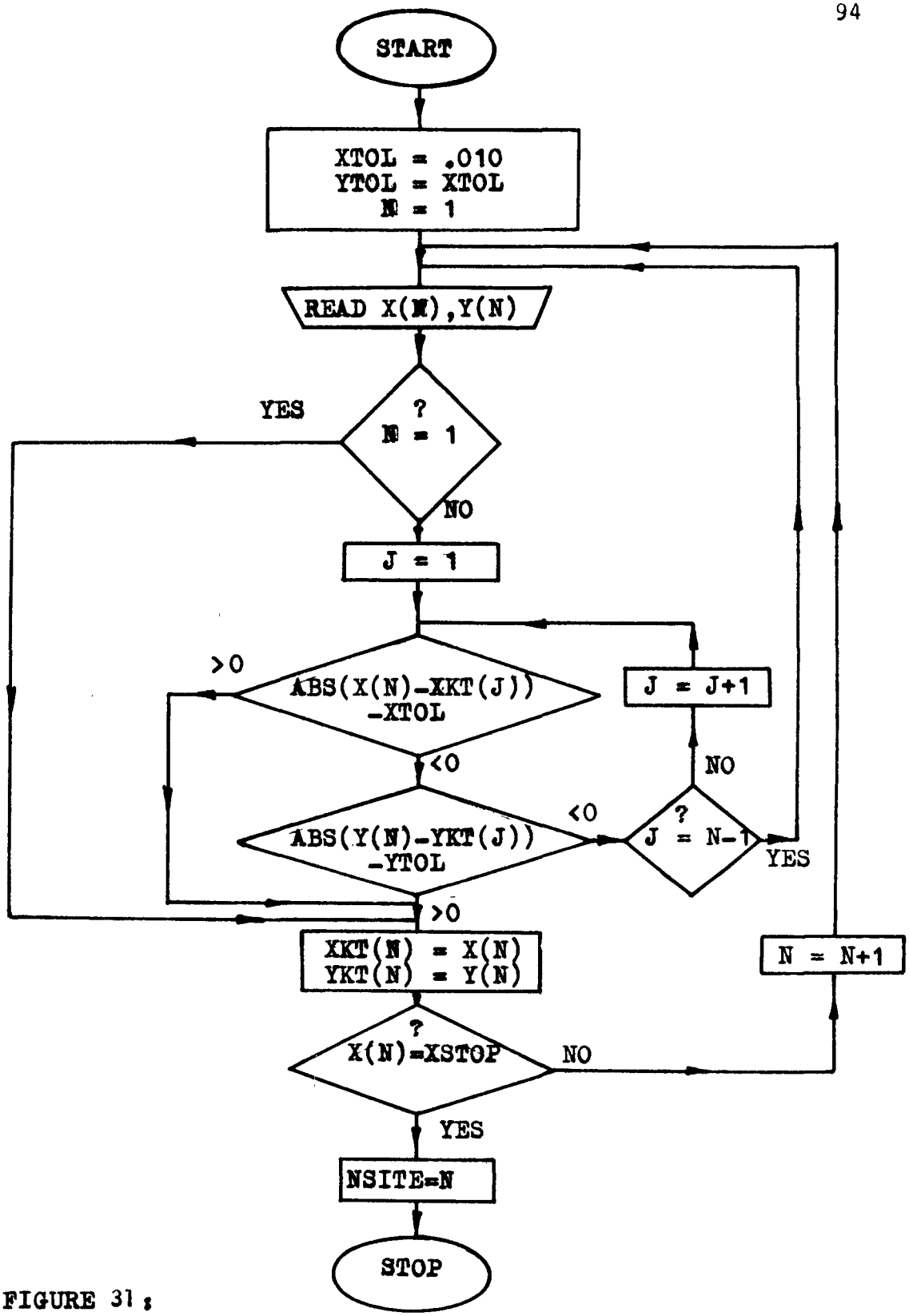

FIGURE 31 :

COMPUTER PROGRAM FOR COUNTING ACTIVE NUCLEATION SITES

A P P E N D I X G

PHOTOGRAPHIC PARALAX TEST

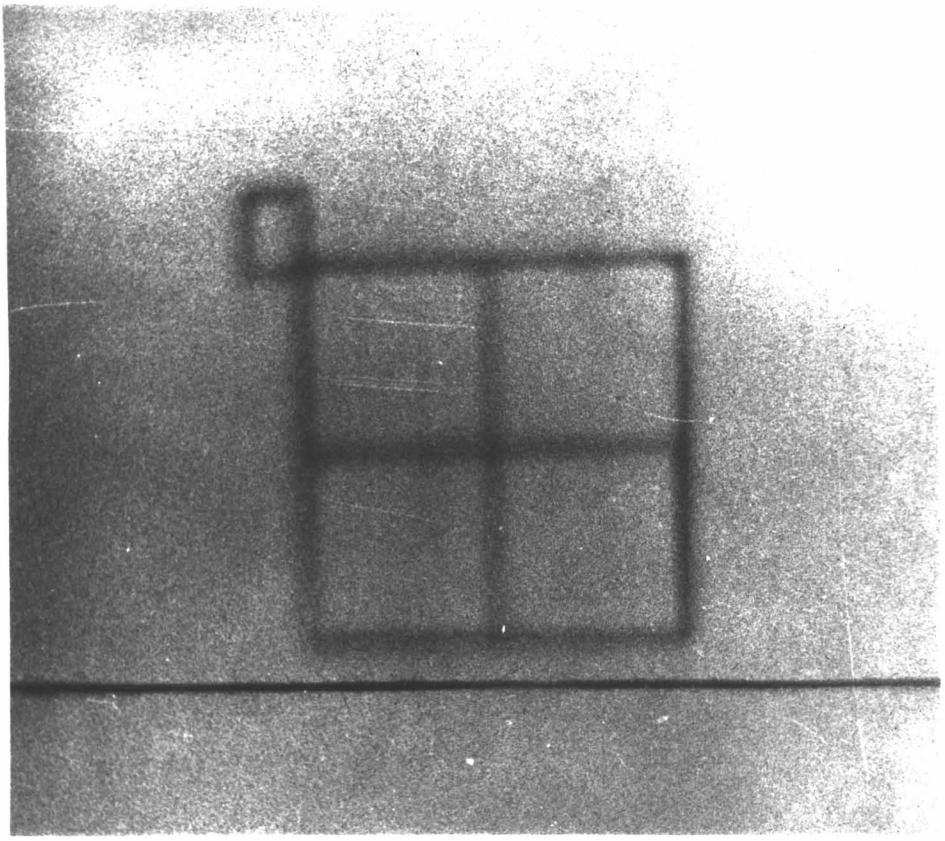

FIGURE 30: PHOTOGRAPHIC PARALAX TEST

Figure 30 is a photograph taken in the same manner as the bubble photographs except in this instance no fluid was present in the test cell. The sharply defined black line is a line drawn on a thin sheet of clear plastic lying on the boiling surface. Also drawn on the thin sheet is a square reference grid identical with the one located on the plastic plate 0.140 inches below the boiling surface.

The grid visible in the photograph is the latter of the two because it is out of focus. The fact that the upper grid is not visible at all indicates that little paralax exists in the system. The width of the out of focus grid lines accounts for approximately one percent of the area represented by the grid and because the upper grid lines lie somewhere behind the out of focus lower grid it is reasonable to assume that paralax can account for no more than one percent error in area.

A P P E N D I X H

TABLE OF FLUID PROPERTIES

TABLE 3

TABLE OF FLUID PROPERTIES

ALL PROPERTIES EVALUATED AT STANDARD PRESSURE.

FLUID	SURFACE TENSION $\frac{DYNES}{CM.}$	DENSITY LIQUID $\frac{LBM}{FT^3}$	DENSITY VAPOUR $\frac{LBM}{FT^3}$	LATENT HEAT $\frac{BTU}{LBM}$	SAT. TEMP ^0F	BURN OUT HEAT FLUX $\frac{BTU}{HR.FT^2}$
FREON 113	19.6	94.26	.4649	63	117.8	64,109
CARBON TETRACHLORIDE	26.8	103.80	.5130	84	170.2	93,550
CHLOROFORM	27.2	97.11	.4781	106	141.0	112,000
DICHLOROETHANE	32.2	81.45	.4066	139	180.1	122,100
TRICHLOROETHANE	33.6	94.02	.4644	109	237.8	110,200

APPENDIX I

EFFECT OF T_w UPON GAERTNER CORRELATION

Effect Of T_W Upon The Gaertner Correlation

An experiment was conducted to test the sensitivity of the Gaertner correlation to changes in the relationship between T_W and N/A. Since in the Gaertner correlation, changes in T_W are deminished by the conversion to the Kelvin scale, concern arose as to whether significant differences in the raw data might be lost when the inverse of T_W cubed was plotted for the Gaertner correlation.

A hypothetical set of data was represented by a straight line superimposed on the data for carbon tetrachloride*. The relationship between T_W and N/A in this test data was such that the slope of the line was one forth that of the line through the actual data. The hypothetical data was then correlated using the Gaertner equation and the slope of the resulting straight line was measured on Figure 21.

It was discovered that a 3 to 1 differential was maintained between the slope of the test data and the slope of the actual data. This indicated that there was a 25 percent reduction in sensativity of the raw data through the use of the Gaertner correlation.

---

* See Figure 16.

While this reduction in sensativity was substantial, substitution of the test data in place of the actual data for carbon tetrachloride was effective in producing a variance ratio in the statistical test of 7.69, which for the degrees of freedom** of the system indicated that the family of slopes was no longer parallel. This fact produced confidence in the sensitivity of both the Gaertner correlation and the variance ratio test.

** Degrees of freedom of numerator = 15
Degrees of freedom of denominator = 4

BIBLIOGRAPHY

1. Gaertner, R. F., "Distribution of Active Sites in Nucleate Boiling of Liquids". Chem. Engr. Progr. Symposium Ser., Vol. 59, No. 41, Pg. 52, 1963.

2. Jakob, Max, and W. Fritz, Forsch. Geb. Ingenieurw., 2,435, 1931.

3. Corty, C. and A. S. Foust, "Surface Variables in Nucleate Boiling," Chem. Engr. Progr. Symposium Ser., Vol. 51, No. 17, Pg. 1, 1955.

4. Bankoff, S. G., paper presented at Am. Inst. Chem. Engrs. Meeting, New Orleans, La., (1955).

5. Clark, H.B., P.S. Strenge, and J. W. Westwater, "Active Sites for Nucleate Boiling", Chem. Engr. Progr. Symposium Ser., Vol. 55, No. 29, Pg. 103, 1959.

6. Kurihara, H.M., and J. E. Myers, "The Effects of Superheat and Surface Roughness on Boiling Coefficients", A.I.Ch.E. Journal, Vol. 6, No. 1, Pg. 83, 1960.

7. Gaertner, R.F., and J. W. Westwater, "Population of Active Sites in Nucleate Boiling Heat Transfer", Chem. Engr. Progr. Symposium Ser., Vol. 56, No. 30, Pg. 39, 1960.

8. Kirby, D.B., and J.W. Westwater, "Bubble and Vapor Behavior on a Heated Horizontal Plate During Pool Boiling Near Burnout", Chem. Engr. Symposium Ser., Vol. 61, No. 57, Pg. 238, 1963.

9. Gaertner, R.F., "Photographic Study of Nucleate Pool Boiling on a Horizontal Surface", Journal of Heat Transfer, A.S.M.E., Transactions, Feb. 1965, Pg. 17.

10. Judd, R. L., "Influence of Acceleration on Subcooled Nucleate Boiling", Doctoral Dissertation University of Michigan, 1968.

11. Clark, P.J., and F.C. Evans, Science, 121, 397, (1955).

12. Hsu, Y.Y., Paper No. 61-WA-177 Am. Soc. Mech. Engrs. Winter Meeting, New York, N. Y. (1961).

13. Gupta, S. S., "Free Convection Heat Transfer From A Heated Horizontal Plate Facing Downwards", Masters Thesis, McMaster University, Nov. 1968.

14. Moroney, M.J., "Facts From Figures", Penguin Books, William Clowes and Sons, 1957.